DM

In-Situ Biosynthesis of Bacterial Cellulose - Porto Santo Clay Composites

Application in drug delivery

MASTER DISSERTATION

Rafael Olegário Sousa Pinto

MASTER IN APPLIED BIOCHEMISTRY

UNIVERSIDADE da MADEIRA

A Nossa Universidade

www.uma.pt

September | 2018

In-Situ Biosynthesis of Bacterial Cellulose - Porto Santo Clay Composites

Application in drug delivery

MASTER DISSERTATION

Rafael Olegário Sousa Pinto

MASTER IN APPLIED BIOCHEMISTRY

SUPERVISOR

Nereida Maria Abano Cordeiro

In-situ Biosynthesis of Bacterial Cellulose-Porto Santo Clay Composites: Application in Drug Delivery

Tese apresentada à Universidade da Madeira com vista à obtenção do grau de Mestre em Bioquímica Aplicada

Rafael Olegário Sousa Pinto

Sob a orientação de:

Professora Doutora Nereida Maria Abano Cordeiro

Faculdade de Ciências Exatas e da Engenharia

Universidade da Madeira

Funchal - Portugal

Setembro 2017

Acknowledgments

I would like to acknowledge everyone that contributed in any way to the execution of my Master Thesis, both at professional and personal level.

To my supervisor, Prof. Doctor Nereida Cordeiro, for all the support and constructive critics which were essential during the development of this project.

To my co-supervisor Marisa Faria for clarifying my questions and for helping me during the execution of this project. I am also grateful to my work colleagues Emanuel Gouveia, Igor Fernandes and Tomásia Fernandes for all the support, motivation given and for making me grow both personally and professionally.

I would like to thank CQM (University of Madeira, Portugal) for providing me the reagents and equipments needed, to Doctor Carla Miguel (CQM, University of Madeira, Portugal) by aiding me with the contact angle measurements and to Dr. Emanuel Gouveia for helping me with the IGC measurements.

To Prof. Doctor Manuela Gouveia (University of Madeira, Portugal) for providing me the orbital agitation incubator and the conditions to make the antibacterial experiments successful.

I would like to thank Doctor Margarida da Costa (Regional Laboratory of Veterinary and Nourishing Security, Madeira, Portugal) for providing me the *Escherichia coli* (*E. coli*) and *Staphylococcus aureus* (*S. aureus*) strains to make the antibacterial studies.

I am also grateful to Prof. Doctor Artur Ferreira (CICECO, University of Aveiro, Portugal) for making the TGA, SEM, EDX and XRD analysis, which substantially increased the quality of the current Master Thesis.

To my friends and colleagues Roberto Aguiar, Dina Maciel, Luis Gomes, Ricardo Mendes, Luisa Ramos and Cláudia Rodrigues for their friendship and motivation.

Finally, I want to do a special acknowledge to my family, particularly to my mother Elisabete and my father Rafael for their unconditional love, support, understanding and concern. A special thanks to my aunt Elsa Silva for her love and encouraging.

Abstract

Bacterial cellulose/clay composites have been lately receiving attention by the scientific community towards drug delivery systems and wound dressing applications. The current work aims to determine the most suitable culture conditions to obtain an effective drug delivery membrane through an environmentally-friendly method. Thus, the BCC composites were synthesized by BC-producing bacteria, *Gluconacetobacter* sp., using an *in-situ* biosynthesis method. *Gluconacetobacter* sp. produced 2.95 g/L BC at optimized culture conditions of 2% glucose, pH of 3.25 and 7 days of cultivation. To obtain the different BCC composites, an agitated culture method was employed. The results show that the introduction of PS clay onto BC obstructed the pores of the synthetized composites, which led into a less porous and more compact material. Additionally, an increase in Υ_s^d (79%), surface basicity ($K_b/K_a \rightarrow 4.2$) and thermal stability (83%) of BC was observed. The composites with incorporated 2% neomycin sulphate were evaluated in terms of their drug release ability and antibacterial activities. These materials exhibited a sustained release up to 24h in a PBS buffer with pH 7.4, whereby they could be used as capsules for oral administration, in the treatment of ileum infections. Furthermore, BCC composites with incorporated neomycin sulphate could be applied as clinical wound healing materials due to their strong antibacterial activities against *Staphylococcus aureus* and *Escherichia coli*.

Keywords: Bacterial cellulose, Clay, Composites, Drug delivery, Antibacterial activity, Inverse Gas Chromatography

Resumo

Os compósitos de celulose bacteriana/argila têm recebido uma grande atenção por parte da comunidade científica para o desenvolvimento de sistemas de libertação controlada de fármacos e aplicação de curativos. Este trabalho visa determinar as condições ideais do meio de cultura para produção de CB, de forma a obter um sistema de entrega de fármacos eficaz através de um método amigo do ambiente. Assim, foram sintetizados compósitos de CB/argila do Porto Santo por bactérias produtoras de CB, *Gluconacetobacter* sp., através da utilização do método de biossíntese *in-situ*. A bactéria *Gluconacetobacter* sp. produziu 2,95 g/L de CB em condições ótimas de 2% de glucose, em um pH de 3,25 e 7 dias de cultivo. Para obter os diferentes compósitos, foi implementada uma cultura em agitação. A introdução de argilas na CB obstruiu os poros dos compósitos sintetizados, o que levou à obtenção de um material menos poroso e mais compacto. Para além disso, foi observado um aumento do Υ_s^d (79%), basicidade da superfície (Kb/Ka → 4.2) e estabilidade térmica (83%) da CB. Os compósitos com 2% de sulfato de neomicina incorporada, foram estudados de forma a avaliar a capacidade de libertação de fármaco e respetiva atividade antibacteriana. Estes materiais apresentaram uma libertação controlada do fármaco durante 24h em tampão PBS com pH 7,4, pelo que poderão ser utilizados como cápsulas para administração oral, no tratamento de infeções do íleo. Além disso, a utilização de compósitos de CB/argila do Porto Santo com sulfato de neomicina incorporado poderão ser aplicados na cicatrização de feridas devido à sua atividade antibacteriana contra a *Staphylococcus aureus* e *Escherichia coli*.

Palavras-chave: Celulose Bacteriana, Argila, Compósitos, Entrega de fármacos, Atividade antibacteriana, Cromatografia inversa gasosa

Index

List of figures

Table of contents

List of abbreviations

γ_s^d – Dispersive component of the surface energy

γ_s^{sp} – Specific component of the surface energy

γ_s^{total} – Total surface energy

A – Adsorption potential

ATP – Adenosine triphosphate

am – Cross section area of the probe molecule

FTIR–ATR – Fourier transformed infrared coupled with attenuated total reflectance

BC – Bacterial cellulose

BCC – Bacterial cellulose/ PS clay composites

CI – Crystallinity index

c-di-GMP - cyclic dimeric guanosine monophosphate

Dp – Diffusion parameter

dTGA – Derivative of TGA

EA – Elemental analysis

E. coli **–** *Escherichia coli*

FID – Flame ionization detector

GC – Gas chromatography

Glc-1-P - glucose 1-phosphate

Glc-6-P - glucose 6-phosphate

GTP – guanosine triphosphate

HS – Hestrin and Schramm culture medium

I_{110} – Intensity of the crystallinity region

I_{am} – Intensity of the amorphous region

IGC – Inverse gas chromatography

NA – Avogadro number

nm – Monolayer capacity

p – Adsorbate pressure

p_0 – Gas pressure

PPi - pyrophosphate

PS clay – PS clay

R – Perfect gas constant

S. aureus – *Staphylococcus aureus*

S_{BET} – Brunauer–Emmett–Teller surface area

SEM – Scanning electronic spectroscopy

SW_{max} – Swelling maximum

SIMS – ion mass spectrometer

TCD – Thermal conductivity detector

TGA – Thermogravimetrical analysis

tR – Retention time

TEM – transmission electron microscopy

UDP–Glucose – Uridine diphosphate glucose

UGPase - UDPGlc pyrophosphorylase

VC – Vegetable cellulose

Vg – Specific retention volume

VN – Retention volume

WCA – Water contact angle

XRD – X–Ray diffraction spectroscopy

Chapter I – Introduction

1.1. Cellulose

In the last years has increased the World concern about the environmental pollution that constitutes a threat to the sustainable development of our planet. Hence, emerged the need to develop new clean and safe chemical processes in order to obtain more biosustainable products. [1] In this context, polymers obtained from renewable sources, such as cellulose, have been widely used instead of traditional polymers derived from petroleum.[2]

Cellulose is the most abundant biopolymer on earth and was discovered in 1838 by Anselm Payen who described cellulose as "*a resistant fibrous solid that remains behind after treatment of various plant tissues with acids and ammonia and after subsequent extraction from water, alcohol and eter*".[3]

This biopolymer is the main component of plant cell walls but it can be also produced by several other organisms, including algae, bacteria and fungi. [4, 5] Although vegetable cellulose and bacterial cellulose (BC) are morphologically different, they have the same chemical structure and the process of synthesis and purification represents a simple and ecologically sustainable solution which can be taken by the industry.[5, 6] Despite the many advantages of using BC, comparatively to vegetable cellulose, the high production cost is one of its major disadvantages. [4, 5]

1.2. Cellulose as a biopolymer

Cellulose $(C_6H_{10}O_5)_n$ consists in a linear homopolymer composed by D-glucose glycosidically linked covalently in a β-(1,4) conformation through acetal functions established between the hydroxyl groups of C1 and C4 carbon atoms. [7-13] Cellobiose is the basic repeating unit of the cellulose polymer, which consists of two glucose anhydride units and where one of the units is round 180º in relation to the plane. [14]

The hydroxyl groups present in cellulose structure form hydrogen bonds between them giving rise to a three-dimensional network consisting of microfibrils that contribute to a greater stability of cellulose. [6, 15, 16] Microfibrils are composed of highly organized

regions (crystalline regions) and regions with greater disorganization (amorphous regions), which arise due to the poor formation of the crystals that make up the three-dimensional network of cellulose. (Figure 1). [17]

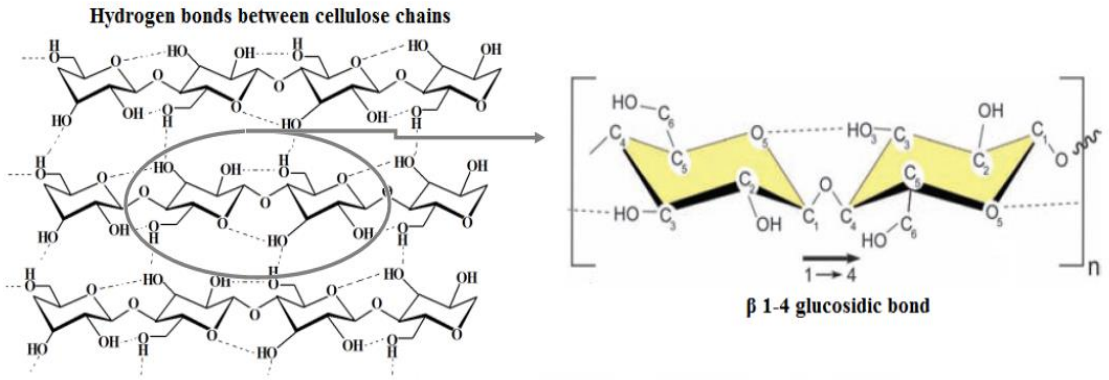

Figure 1: Linear structure of cellulose (n = degree of polymerization). Reproduced from Poletto *et al* (2013). [18]

The majority of cellulose synthesis occurs in the cell wall of plants, being associated with lignin and hemicelluloses, however, it may have a bacterial, animal, chemical or enzymatic origin. [19, 20]

Cellulose can be found under two distinct forms of crystallization: cellulose I and cellulose II. In cellulose I, the glucose chains are oriented in parallel, which makes it a thermodynamically unfavourable structure whereas in the cellulose II the glucose chains are antiparallel since it has hydrogen bonds complementary to each monomer of glucose. [7, 10, 21, 22]

Cellulose I exhibit two main different crystalline forms, cellulose I_α and I_β. Cellulose I_α is crystallized in large nanofibrils.[23] Cellulose I_β is characterized by the formation of smaller nanofibrils which, however, make the structure of the cellulose I_β more thermodynamically stable. [23] In addition, the two allomorphic forms differ from their unit cell. The I_α cellulose exhibits a triclinic unit cell whereas the I_β cellulose exhibits a monoclinic cell. [23]

1.3. Bacterial cellulose (BC)

Adrian J. Brown discovered in 1886 a gelatinous membrane with a similar chemical structure as plant cellulose cell wall, as a product of microbial fermentation of acetic acid obtained from the ”vinegar plant”. [20, 24] The “mother vinegar” had the ability of producing a “*jelly-like translucent mass on the surface of the culture fluid; this growth rapidly increases until the whole surface of the liquid is covered with a gelatinous membrane, which, under very favourable circumstances, may attain a thickness of 25 mm*”. [25] This gelatinous membrane was denominated as bacterial cellulose and the “vinegar plant” as *Acetobacter xylinum*. [25] Nowadays, the vinegar plant was reclassified taxonomically as *Gluconacetobacter xylinum*. [26]

BC is produced by a wide variety of microrganisms of the *Acetobacteraceae* family, namely the *Gluconacetobacter* genus.[27] The bacteria of this family have the ability to convert ethanol to acetic acid and can also grow at low pH levels.[27] *Gluconacetobacter* sp. is one of the most common acetic acid bacteria characterized by their ability to produce cellulose, which represents not only an environment-friend process, but also adds value to the final product. [27, 28]

Gluconacetobacter sp. is known as a Gram-negative bacteria, strictly aerobic, non photossynthetic, which has the ability of producing cellulose in great abundance.[19] It has a morphology in the form of straight or slightly curved and elongated rods of a size ranging from 1.0 - 4.0 x 0.6 - 0.8 µM and it can be found in fruits, vegetables, vinegar or alcoholic beverages. [19, 24, 26]

The main advantage of cellulose production by bacteria of the genus *Gluconacetobacter* is the wide variety of substrates on which it can grow and its ability to convert different substrates into cellulose, such as glucose, fructose, glycerol or other organic substrates.[4] BC biosynthesis by *Gluconacetobacte*r genus has been strictly linked to the cell metabolism. As a matter of fact, culture media conditions are determinant for BC production by regarding carbon and nitrogen sources, temperature, pH and reactor type.[29] BC can also be synthesized by *Agrobacterium*, *Aerobacter*, *Achromobacter*, *Azotobacter*, *Rhizobium*, *Sarcina*, *Pseudomonas*, *Alcaligenes, Zoogloea* and *Salmonella*. [17, 24]

At the structural level, BC is very similar to vegetable cellulose, differing in fiber width (less than 100 nm).[1] In addition, it has unique physical and mechanical properties: high crystallinity, higher mechanical strength, *in situ* moldability, higher water absorption and retention capacity, high elasticity and a higher degree of purity since it is not associated with lignin and hemicelluloses. [24] Table 1 shows some of the properties of BC and its comparison with the properties of vegetable cellulose.

Table 1: Properties of vegetable cellulose and bacterial cellulose. Adapted from Pecoraro *et al* (2008).

Properties	**Vegetable cellulose**	**Bacterial cellulose**
Fiber Width	1.4 – 4.0 X 10^{-2} mm	70 – 80 mm
Crystallinity	56 – 65%	65 – 79%
Degree of polymerization	13000 – 14000	2000 – 6000
Young Modulus	5.5 – 12.6 GPa	15 – 30 GPa
Water content	60%	98.5%

The use of BC by the industry has been an evolutionary milestone in the world evolution due to its excellent mechanical properties and its stability in the interaction with high temperatures and with chemicals, being widely used as reinforcement/support material in biomedical devices, in the cicatrization of wounds, tissue regeneration and in the textile industry. [31-35]

The potential utilization of BC can be increased if substances capable of incorporating into the cellulose fibers are added, such as amino, carboxylic and hydroxyl groups. [36]

The most commonly used carbon source in the synthesis of BC is glucose, however, other substrates which have the ability to produce BC have been used, such as mono and disaccharides, alcohols and carboxylic acids. [4]

1.4. BC Biosynthesis

The synthesis of BC is an expensive process for the cell, consuming about 10% of the ATP generated by bacterial metabolism.[17] In addition, the energy used in the synthesis of bacterial cellulose comes from an aerobic metabolism, so that the oxygen is required to the growth of bacteria. [17]

Biosynthesis of BC either by *Gluconacetobacter* sp. or by other cellulose-producing organisms involves several steps that are specifically regulated by various enzymes. This is essentially based on two distinct steps: the polymerization of glucose molecules into β-1,4-glucan chains and the packaging and crystallization of the cellulose chains. In the first step the cellulose precursor, the uridine diphosphate glucose (UDPGlc) is synthesized, whereas in the second step polymerization of glucose chains is performed which combine to form microfibrils by hydrogen bonding and van der Waals forces. Consequently, a three-dimensional network is formed which presents several empty spaces between the fibrous structure, allowing the BC to present a larger surface area that favors the formation of a matrix with a high porosity. [7, 10, 17, 30]

Bacterial cellulose is synthesized between the exterior and the cytoplasmic membrane of cells.[37, 38] The cellulose molecules are synthesized inside the bacteria and then twisted to form protofibrils 2-4 nm in diameter. It is from protofibrils that microfibrils are constructed which are then packaged to form fibers of approximately 80 nm in the form of rolled strips. [37, 38]

During the BC biosynthesis process, various carbon compounds in the culture medium, such as glucose, are used by the bacteria and then polymerized into β-1,4-glucan chains and finally secreted outside of the cells through pores located on its outer membrane. [39]

The synthesis of BC by *Gluconacetobacter* sp. from a specific substrate, namely glucose, can occur through two metabolic pathways: the phosphate pentose pathway which allows the oxidation of carbohydrates and the Krebs cycle which allows the oxidation of fat acids. Thus, bacterial cellulose is obtained from a phosphate hexoses metabolism sustained directly by the phosphorylation of exogenous hexoses and indirectly by the pentose phosphate pathway or by the Krebs cycle, associated with

gluconeogenesis.[10, 17] Despite this, *Gluconacetobacter* sp. is incapable of metabolizing glucose anaerobically due to the absence of an enzyme necessary for the performance of glycolysis, phosphofructokinase.[37] In figure 2, the metabolic pathways necessary for the synthesis of BC and the process of construction of BC nanofibers are segmented.

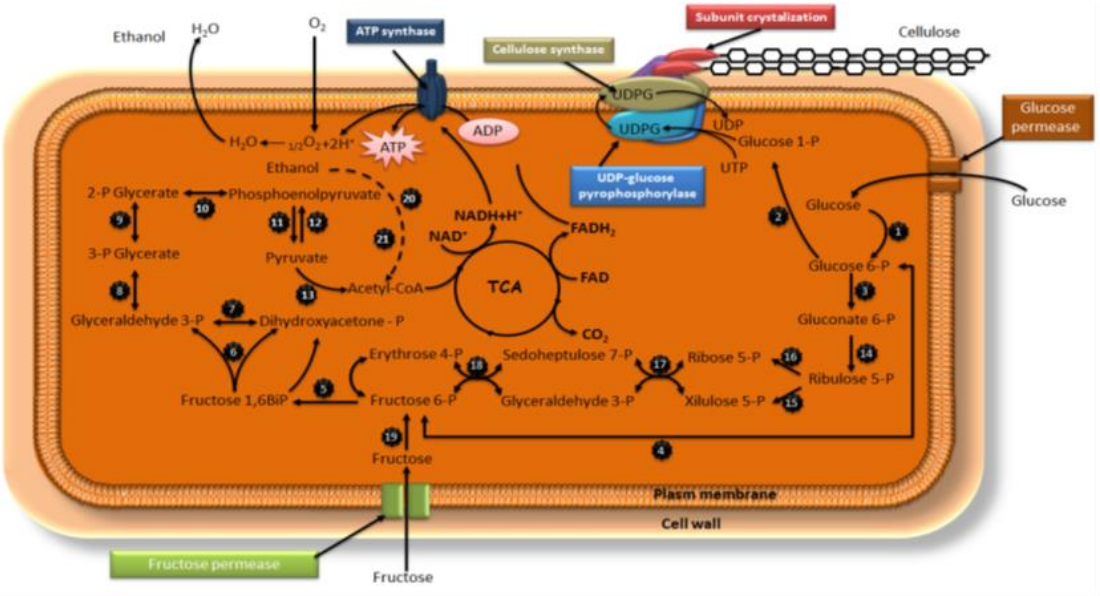

Figure 2*:* Schematic representation of the metabolic pathways associated with the synthesis of *Gluconacetobacter sp.* and the construction of nanofibrils. Reproduced from Lustri *et al* (2015).

For glucose to be converted to cellulose four fundamental enzymatic steps should be followed. The first step is based on phosphorylation of glucose transported from the outside to the cytoplasm, giving rise to glucose 6-phosphate (Glc-6-P) by glucokinase. The next two steps include isomerization of glucose 6-phosphate to glucose 1-phosphate (Glc-1-P), phosphoglucomutase and conversion of Glc-1-P to UDPGlc by UDPGlc pyrophosphorylase (UGPase). The last step consists of the incorporation of units of UDPGlc into β-1,4 glycosidic chains through an enzyme located in the cytoplasmic membrane, cellulose synthase. [17, 37]

Cellulose synthase is a protein complex consisting of 3 (AxCcSAB, AxCcSC and AxCcSD) or 4 (AxCcSA, AxCcSB, AxCcSC and AxCcSD) protein subunits encoded by genes present in the chromosomal operon, called MCs.[17]

In *Gluconacetobacter*, bis- (3'- 5') – cyclic dimeric guanosine monophosphate (c-di-GMP) plays an important role in cellulose biosynthesis since it acts as an allosteric activator of cellulose synthase.[37] In the absence of c-di-GMP, the cellulose synthase remains inactive or exhibits a low enzymatic activity.[37] The balance between c-di-GMP in the free or bound form is modulated from the concentration of intracellular potassium.[37] The level of free c-di-GMP is regulated by two specific enzymes, diguanylate cyclase (DGC) that cycles two molecules of GTP under the release of pyrophosphate (PPi), and phosphodiesterase A.[17]

The cellulose synthase activity can be disrupted by c-di-GMP phosphodiesterases A and B (PDE-A and PDE-B).[40] Phosphodiesterase A is responsible for the breakdown of c-di-GMP and the formation of pGpG which is then degraded so that two 5'-GMP molecules are formed.[40] The activity of PDE-A can be inhibited by the presence of Ca^{2+}. [40]

1.5. Static and agitated biosynthesis

BC can be synthesized from two distinct processes: agitated or static culture, the latter being the most traditional. [7]

Throughout static culture BC is produced at the liquid-air interface of the culture medium as a result of the packaging of crystalline and crosslinked fibers which form a film or gel which increases in thickness with increasing culture time. [10, 30, 41-44] The formed film grows downwardly until all the cells incorporated become inactive or die due to the oxygen deficit. In the agitated culture, fibrous suspensions, spheres or small BC pellets with irregular shapes are produced. From this process the bacteria are capable of having a faster growth however, they produce a smaller amount of BC. [10, 30, 41-44] The pellets formed have a lower degree of polymerization, mechanical strength and crystallinity when compared to those produced by static culture. In spite of this, the process of producing BC through shaking culture is much faster and allows to obtain a higher cell density and a greater contact with the oxygen. [30]

The choice between synthesis by agitation or in static culture is dependent on the final destination and its applications, since its morphology and its physical and mechanical properties depend on the culture method. [44] Static culture has already been extensively studied and bacterial cellulose synthesized as a membrane has a wide range of

commercial applications in many areas, including food, textile, biomedical and pharmaceutical industries. The membrane formed could be molded during the biosynthesis process so that the desired shape and size is obtained, depending on the conditions under which the cellulose is subjected. [39] From a vigorous treatment at high temperatures and with strong bases, such as sodium hydroxide, it is possible to remove cells embedded in the cellulose fibers and to obtain a non-toxic, non-pyrogenic and biocompatible biomaterial. [39]

Already the agitated culture is more indicated for large scale productions due to the greater productivity in theoretical terms. The main disadvantage of this method of cultivation is the high probability of the appereance of mutant species that are unable to synthesize cellulose (Cel^-) and that are responsible for the decrease in productivity. [44] The appearance of these non-mutant species was described by Hestrin and Schramm [45] which, after isolating different types of *Gluconacetobacter* xylinum cells, distinguished species with the ability to produce cellulose (Cel^+) and non-cellulose (Cel^-) species. Cel^+ type colonies are spherical, convex, gelatinous and with smooth ends whereas Cel^- type colonies are irregular, flat, viscous and with wavy ends. [44]

1.6. BC applications

BC has been used in various products in a wide spectrum of areas, including the food industry, textiles, cosmetics, bioengineering and papermaking, among others. Its high mechanical strength, purity, water retention capacity and large surface area are some of the properties that have made its use so intensive. [6, 7, 46]

Nevertheless, it is in the biomedical industry that BC has been more applied, namely in tissue engineering.[9] In this area, several studies have been done on the use of BC as artificial skin in wound healing [47], dental implants [48] and in the controlled release of drugs. [7]

In the food industry, BC has been used in the production of healthier foods such as nata de coco which was the first one commercialized. Nata de coco is produced mainly in the Philippines and is obtained after dicing, washing and immersion in sugar syrup. [49, 50] After this process, it can be served in desserts, fruit cocktails and jams.[50]

Furthermore, bacteria of the genus *Gluconacetobacter* sp. present the ability to establish a symbiosis with yeasts in tea extracts to form an acidified medium that could be consumed as Kombucha tea with the purpose of improving health. BC can also be used as a thickening and gelling agent in processed foods. [7, 51]

Moreover, BC has been used in the paper industry [21, 52] and in the development of biodegradable food packaging due to its selective permeability. [53, 54] In the area of electronics, BC has been tested on loudspeakers and headphones.[47]

1.7. BC composites

Although BC presents unique properties, there are some limitations that restrict its applicability, for example: the absence of antibacterial properties, optical transparency and ability to withstand stress. [50]

The biomedical efficacy of BC can be increased by the synthesis of composites, by the incorporation of bioactive molecules.[30] The new BC composites give bacterial cellulose excellent conductive, magnetic, optical, antibacterial, anti-viral and antifungal properties, biocompatibility and a greater capacity for wound healing purposes.[30]

Composites were first defined in the 1980s by Roy *et al* as a compound composed of several phases and in which one of the phases has a nanometric scale length. As early as 1992, Kormarneni defined composites as composites with more than one Gibbs solid phase where at least one of the dimensions lies at the nanoscale and where the solid phases have a length between 1 and 20 nm. [55]

In the preparation of composites of BC, several approaches have been developed, including the incorporation of bioactive molecules in the culture medium during BC biosynthesis, the *in-situ* polymerization of monomers in the BC three-dimensional network and the blend with other polymeric materials. The first strategy referred above is based on the synthesis of *in situ* composites, which is described in detail below. [31, 56-59]

1.7.1. Synthesis of BC composites by *in situ* biosynthesis

One of the strategies for the synthesis of composites is based on the introduction of compounds of interest in the culture medium during the BC biosynthesis process. Thus,

it is possible to synthesize composites at the same time as the bacterial cellulose fibers are produced, by incorporation of these compounds. Various compounds/polymers have been incorporated into the culture medium so that composites are obtained, such as: glyoxal [31], silica nanoparticles [38], poly (vinyl) alcohol [56], chitosan [57], collagen [60], hydroxyapatite [61] and calcium carbonate. [62]

According to Luo *et al* [60] was synthesized a bacterial cellulose/collagen (BC/COL) nanocomposite for application in the tissue engineering area by incorporating collagen into the culture medium.[60] This nanocomposite presented a higher thickness and greater porosity when compared to BC (Figure 3). It also caused an increase in the synthesis of BC since it functions as a source of carbon and nitrogen. [60]

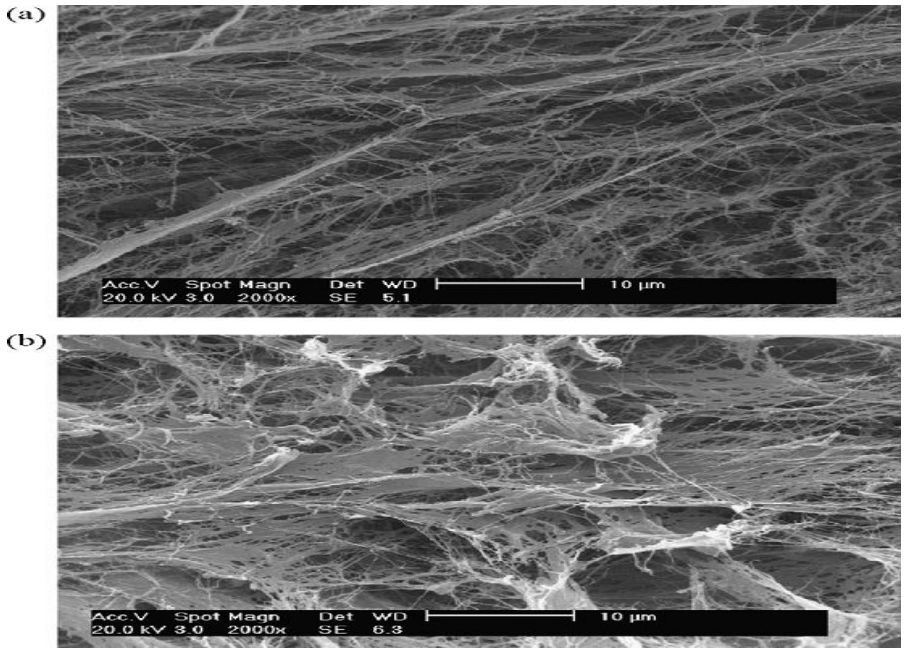

Figure 3: SEM image of BC (**a**) and of BC/COL nanocomposite (**b**). Reproduced from Luo *et al* (2008)

A new nanocomposite of BC/aloe vera was described by Saibuatong *et al* [58] by incorporating different concentrations of aloe vera into the culture medium during BC biosynthesis.[58] The combination of BC and aloe vera allowed the improvement of mechanical properties, water retention capacity, water vapor transmission rate and degree of crystallinity. The new nanocomposite of BC/aloe vera obtained showed better mechanical properties and biocompatibility, which makes this a suitable material for use in the biomedical area.[58]

Already Castro *et al* [56] synthesized a novel BC/PVA nanocomposite by addition of PVA to the culture medium, followed by chemical cross-linking.[56] This process prevented the PVA matrix from being lost during the purification of the membranes, which promoted an improvement in the properties of the composites as a result of the interaction between the PVA matrix and the bacterial cellulose.[56]

According to Phisalaphong *et al* [57] it was developed a new nanocomposite of BC/chitosan by incorporation of low molecular weight chitosan into the culture medium.[57] This nanocomposite exhibited a dense and homogeneous fibrous structure with a larger surface area and pores with a smaller diameter. [57]Although the addition of chitosan altered these properties, it did not modified BC properties, such as the degree of crystallinity and the antimicrobial activity. [57]

1.8. Incorporation of PS clay

Biosynthesis of BC coupled with the incorporation of bioactive compounds allows composites to be obtained in "*only one-step*", which represents an added value that allows them to be used in a wide range of applications, namely in the biomedical and cosmetic fields.

Clays are fine-grained minerals that have a spherical diameter of <2.0 μM and a density of approximately 2.65 g/cm^3.[63] These are essentially constituted by layered magnesium or aluminium silicates composed of tetrahedrally coordinated silicate sheets and octahedrally coordinated magnesium or aluminium hydroxide sheets (Figure 4).[64] Clays are often used for therapeutic and cosmetic purposes since drug molecules can be encapsulated between the inner layers through ion exchange processes. [64, 65]

The role of clay in human health has grown exponentially due to the advances obtained in modern instrumentation such as field emission scanning electron microscopes (FESEM), transmission electron microscopes (TEM), atomic force microscopes (AFM) and ion mass spectrometers (SIMS) which allows the study of surfaces of nano-scale minerals *in situ* within their natural environmental matrix.[63]

Clays are commonly used by the biopharmaceutical industries as oral medication ingredients for antacids, gastrointestinal protectors, antidiarrheics and as topical medication ingredients for dermatological protectors, anti-inflammatories and local

anesthetics due to their amphoteric behavior, porosity, high swelling capacity and surface area. [64, 66]They have also been widely used in the treatment and cure of cancer, ulcers, cysts, tumors and osteoporosis due to their high surface area, absorption and heating capacity, and in the synthesis of inorganic materials with antibacterial properties due to their cation exchange ability. [63] Additionally, clays can be used to remove oils, secretions, toxins and contaminants from the skin due to their extremely fine particle size.[63] Clay composites have been developed for wound healing purposes due to their efficacy in sustainable drug releases.[66]

Clays may be considered healing compounds once they present many natural features of their nanometric mineral assemblages that are therapeutic and promote health.[67] The practice of consuming clays by humans and animals (geophagy) can promote nutrition by providing salts and micronutrients and provides ailments and hunger relief. They have been widely used in pelotherapy (mud baths) for many years and in wound care to stop bleeding since it has the capacity to adsorb fluids and protect the skin.[67]

Clays found in Porto Santo island, in the Madeira archipelago, are smectite clays widely used in facial masks due to their impressive moisturizing, astringent and antiseborreic properties.[68] Porto Santo clay (PS clay) are mostly constituted by ferrous minerals, calcite, feldspars, phyllosilicates and smectite which in turn are composed by cations such as calcium, sodium, potassium, and magnesium.[69, 70] They are also composed by other minority compounds resulting from a higher contact with the sea namely: iron oxide from magnetite, copper, chromium, cobalt, nickel, zinc, vanadium, cerium, uranium, arsenic and strontium. The last one is a mineral which exists in great abundance in Porto Santo's seawaters. [69, 70]

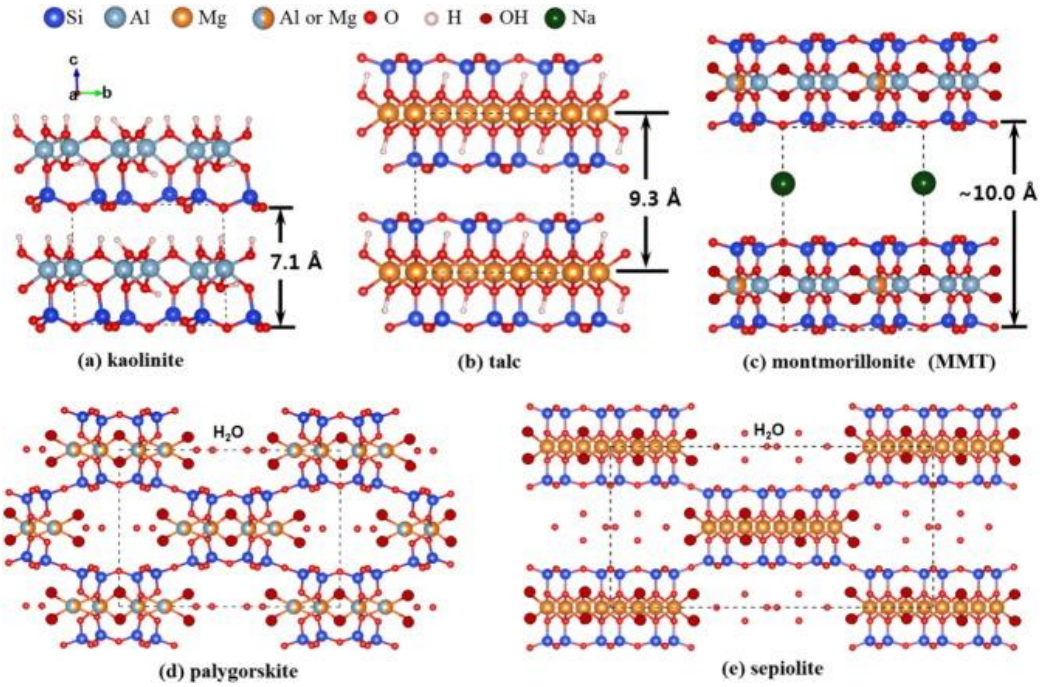

Figure 4: Crystalline structure of some often-used clays for therapeutic purposes. Reproduced from Yang *et al* (2016).

1.9. Inverse gas chromatography (IGC)

In the last few years, inverse gas chromatography (IGC) has been widely used in the characterisation of the surface properties of non-volatile materials, mainly organic and inorganic materials such as polymers and drugs and silica, respectively.[71-73] This is a technique that offers several advantages, namely its sensivity, reproducibility, simplicity, requires low amounts of material, can be run at a wide range of temperatures and does not require pure solutes. [74, 75] Unlike in gas chromatography (GC) the stationary phase is the sample under investigation while a substance (gas carrier) in the mobile phase is used as a probe molecule (Figure 5).[74, 76]

In the IGC method, the dispersive energy and the acid-base parameters of polymer surfaces can be evaluated by injecting n-alkanes and polar probes at infinite dilution on a column packed with polymer material. The dispersive energy and the acid-base characteristics of polymer surfaces have been commonly used to measure the surface activity of polymers, to estimate the behaviour of polymers in water and to evaluate the biodegradability of polymers.[77]

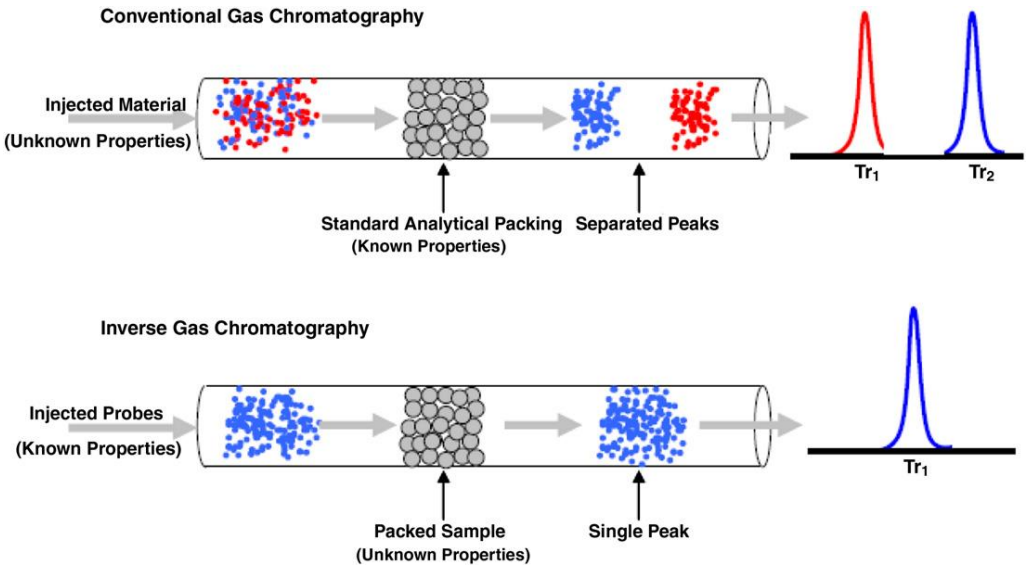

Figure 5: Schematic representation of conventional GC and IGC. Reproduced from Cordeiro *et al* (2013).

1.9.1. IGC instrumentation

IGC consists of a mass flow controller composed by two ovens, one for the solute reservoir and another for the column with the packed sample, two detectors and a computer.

Helium is used as the carrier gas once it is inert, which is crucial to avoid interactions with the column and the adsorbate. Since the analysis is conducted at infinite dilutions, the adsorbate-adsorbate interactions are neglected.[78]

IGC is equipped with two detectors: flame ionization detector (FID) and thermal conductivity detector (TCD). The flame ionization detector (FID) contrary to TCD, is better suited under infinite dilution tests since it has a higher sensivity, up to 10^{-9} mol. [79] Both can detect organic molecules while FID, unlike TCD, cannot detect water.[79]

In chromatography, retention time (T_r) is commonly used in the characterization of the peaks, although it changes considerably according to the experimental conditions, such as the carrier gas flow rate and the pressure drop in the column.[80] This is of great importance since in chromatography the volume of the gas changes when it crosses the column, due to its compressibility property. The James–Martin compressibility factor (j)

takes into consideration the inlet and outlet pressure of the carrier gas in the column, correcting the pressure variations along the run. [80]

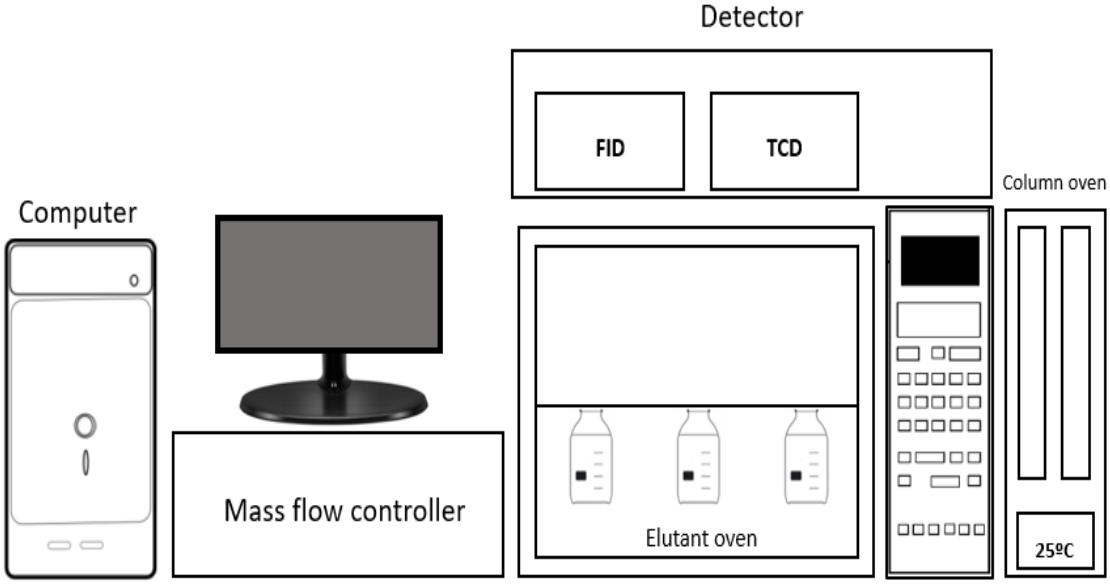

Figure 6: Schematic representation of the inverse gas chromatography apparatus.

Retention volume (VN) considers the parameters discussed above and offers more reliable and reproducible results. [81] Adapting to IGC, VN can be defined as the volume of the mobile phase that left the column during the time the adsorbate was interacting with the analyte. Therefore, VN can be used as a reference parameter since it is affected by the interactions between the adsorbate and the sample.[81] Other parameters such as the temperature and the sample mass can also be taken into consideration.[82] Thus, the values of VN can be normalized, being called specific retention volume (Vg). It can be deducted from the following equation (1):

$$\mathrm{Vg} = \frac{\mathrm{F.j}}{\mathrm{m}} . (T_r - t_0) . \frac{273.15}{\mathrm{T}} \qquad \text{(Equation 1)}$$

1.9.2. Surface energy

1.9.2.1. Dispersive component

The surface of a solid is composed of free bonding functional groups, which establishes an interface with the surrounding environment. The free energy of a solid's surface is an important parameter, defined as the energetic difference between the surface and the bulk per unit area of surface. According to Fowkes, surface energy interactions can be split in dispersive forces (Van der Waals interactions) and specific forces, such as acid–base, hydrogen bond and metallic interactions.[83] From the injection of a series of *n*–alkanes, Schultz *et al*. determined the dispersive component [84], by applying the following equation (2):

$$\Delta G^d = \mathrm{RT}\ln(\mathrm{Vg}) = 2\,N_A.(\gamma s^d)^{\frac{1}{2}}.\mathrm{am}(\gamma L^d)^{\frac{1}{2}} + \mathrm{K} \qquad \text{(Equation 2)}$$

where ΔG^D is the Gibbs free energy of adsorption of the dispersive component; R the perfect gas constant; N_A the Avogadro's constant; a_m the cross–sectioned area of the adsorbate; Υ_s^D the dispersive component of the material's surface energy; Υ_L^D the probe surface tension and K a constant.

From the previous equation, one should obtain a linear trend in the data, usually designated as the alkane line, being the slope equal to $2\mathrm{N_A}.\sqrt{\gamma \mathrm{s^d}}$. Basically, a probe with a certain $a_m\sqrt{\gamma}s^d$ will have a given ΔG^d which corresponds to the vertical distance between the x axis and the data plotted.[74]

1.9.2.2. Specific component

In the case of polar molecules, the free energy of absorption is above the alkane line, since both dispersive and specific interactions take place between the surface of the sample and the adsorbate, corresponding to the vertical distance between the polar adsorbate and the alkane line.[74] From the specific free energy of adsorption, it is possible to obtain the surface donor (Υ_s^-) and acceptor (Υ_s^+) numbers, based on the Good–Van Oss concept. Experimentally, two probe polar molecules should be used: one acid and one

basic. [85] This way, it is possible to obtain the parameters referred above from the following equation (3):

$$\Delta G^{sp} = 2\, N_{A\, a_m} \left(\sqrt{\gamma s^{-}\, \gamma L^{+}} + \sqrt{\gamma s^{+}\, \gamma L^{-}}\right) \qquad \text{(Equation 3)}$$

Where Υ_L^+ and Υ_L^- are the acceptor and donor numbers of the adsorbate and ΔG^{sp} the Gibbs specific free energy of adsorption.

After obtaining the donor and acceptor numbers of the surface, it is possible to estimate the specific free energy of adsorption from the following equation (4):

$$\Upsilon s^{sp} = 2\sqrt{\gamma s^{-}\gamma s^{+}} \qquad \text{(Equation 4)}$$

Now with both dispersive and specific surface energy, it is obtained the total surface energy (Υ_s^{Total}), corresponding to the sum of the two components (Equation 5).

$$\gamma s^{Total} = \gamma s^{d} + \gamma s^{sp} \qquad \text{(Equation 5)}$$

1.9.3. Acid-base character according to Gutmann Method

Concerning the specific component of the surface, a different approach was taken by Gutmann. Likewise, the Good–Van Oss method previously described, the adsorbates also have reference values, which are obtained experimentally. For the basic component, the donor number (DN) is defined as the enthalpy of interaction between the molecule being studied and $SbCl_5$ (Lewis acid) in 1,2–dichloroethane, a neutral solvent. On the other hand, for the acid component, the acceptor number (AN) was determined by correlating the induced chemical shifts in 31P NMR spectra of triethylphosphine oxide (Lewis base) dissolved in the acid molecule being studied. According to Riddle and Fowkes these chemical shifts can be influenced by Van der Waals interactions, which could improve the method by developing modified acceptor numbers (AN*).[86] By doing so, the donor and acceptor numbers can be compared and related to surface acidity and basicity from the following equation (6):

$$\frac{\Delta G^{sp}}{AN*} = \frac{DN}{AN*} \times \mathrm{K_A} + \mathrm{K_B} \qquad \text{(Equation 6)}$$

being K_A and K_B acid and basic constants that characterize the polarity of the surface. By plotting the results with the previous equation, the slope should correspond to K_A while K_B to the interception with the Y axis.

1.9.4. Surface area

Surface area (S_{BET}) of materials are commonly obtained from the Nitrogen adsorption isotherm at 77K, using the Brunauer–Emmett–Teller (BET) equation.[87] This method is based on the relationship between the amounts of gas adsorbed at different gas pressures, at a constant temperature. After a certain amount of gas pressure, the amount of gas adsorbed reaches a plateau, physically corresponding to the monolayer capacity (n_m). Through IGC, these parameters can be evaluated and therefore it is possible to determine the surface area of the samples. According to Brunauer *et al* the original equation is linearized (7), being possible to determine the monolayer capacity from the slope and the intercept.

$$\frac{p}{n\,(p_{0-p}\,)} = \frac{c-1p}{n_m\,c\,p_0} + \frac{1}{n_m\;c} \qquad \text{(Equation 7)}$$

being p_0 the gas pressure, p the adsorbate pressure, n_m the monolayer capacity, n the amount of probe adsorbed and c a constant.

If the area of the probe used in the BET measurements is known, it is possible to obtain the BET surface area (S_{BET}) by the following equation (8):

$$\mathrm{S_{BET}} = a n_{m\,N_A} \qquad \text{(Equation 8)}$$

1.9.5. Surface heterogeneity

Using the sorption isotherm results it's possible to calculate the adsorption potential distribution, which will correspond to the energy profile of the surface. [88]

Firstly, to obtain the distribution function, partial pressures are converted into the adsorption potential (A) from the following equation (9):

$$\mathrm{A} = \mathrm{RT} \ln\left(\frac{p}{p_0}\right) \qquad \text{(Equation 9)}$$

Then, the distribution parameter (Φ) is determined, corresponding to the 1st derivative of the adsorbed amount with the adsorption potential, which will give us the energy profile plot.

1.9.6. Diffusion analysis

In diffusion analysis, different flow rates of mobile gas are used. The principle behind this procedure is that as the probe progresses from the inlet to the outlet, it spreads due to diffusion phenomena.[89] The diffusion coefficient can be obtained from the width of the elution peak through the equation developed by van Deemter *et al* as shown in equation 10.

$$\mathrm{H} = \mathrm{A} + \frac{B}{u} + \mathrm{Cu} \qquad \text{(Equation 10)}$$

where H is the height equivalent to the theoretical plate (cm) and u is the carrier gas speed (cm/s). The parameters A, B and C are independent of the velocity of the carrier gas, related to the column, gases and operating conditions, respectively.[89, 90] The parameter A is called eddy diffusion and is related to the size of support particles and irregularity of packing. [91] The parameter B describes the longitudinal diffusion of the probe along the stream of carrier gas.[91] The parameter C is related to peak broadening which is due to the mass resistance within the column. [91] Through the constant C it is obtained the diffusion coefficient (Dp) through the following equation (11):

$$\mathrm{C} = \frac{8}{\pi} \frac{K}{(1+K)^2} \frac{d^2}{Dp} \qquad \text{(Equation 11)}$$

where K is the partition ratio and d the film thickness.

Aim of the study

The main purpose of this work was the development of an *in-situ* biosynthesis process to produce composites with bioactive properties using a green chemistry strategy in only one-step to reduce the consume of solvents and obtain biocompatible, biodegradable and an environmentally friendly material. [31, 58, 92]

The focus of the current work was the production of bacterial cellulose/PS clay composites (BCC) with potential use as drug delivery systems, for the treatment of ileum infections. For this purpose, optimum culture medium conditions for bacterial cellulose (BC) production by *Gluconacetobacter* sp. were studied, namely inoculum density, pH, temperature, glucose concentration and production time. After optimizing the culture conditions for BC production, different BCC composites were produced under an agitated culture medium. Then, the BC and BCC composites were evaluated in terms of their structural, morphological and surface characteristics through Fourier transformed infrared coupled with attenuated total reflectance (FTIR–ATR), scanning electronic microscopy (SEM), elemental analysis (EA), X-ray diffraction (XRD), thermogravimetrical analysis (TGA), swelling, contact angle measurements and Inverse Gas Chromatography (IGC). Finally, the BCC composites were tested in terms of drug loading and release capacities and antimicrobial activity on *Escherichia coli* and *Staphylococcus aureus*, using neomycin sulphate as the reference drug.

Chapter II - Materials and Methods

2.1. Preparation of culture medium

The culture medium used for the production and maintenance of *Gluconacetobacter* sp. was standard Hestrin and Schramm (HS) culture medium containing glucose (2%, w/v), bacterial peptone (0.5%, w/v), yeast extract (0.5%, w/ v), di-sodium hydrogen phosphate (0.27%, w/v) and citric acid (0.115%, w/v). The medium was autoclaved at 121°C for 15 minutes and the pH adjusted to 5.0 with ethanol (1%, v/v) and acetic acid (0.4%, w/v).

2.2. Inoculum preparation

The bacterial suspension used to inoculate the culture media was prepared from a single colony withdrawn from the solid HS medium and cultured for 48h in liquid HS medium under static conditions, at 22^{o}C. An initial inoculum with 10% (v/v) was prepared for all the experiments, under aseptic conditions. The absorbance of the inoculum was adjusted to 0.4.

2.3. Optimization of culture conditions

Since our isolate *Gluconacetobacter* sp. is known to produce BC, various nutritional parameters such as the concentration of sugar along with physical parameters such as inoculum ratio, pH, temperature and production time were studied to obtain the optimum culture conditions for maximum BC production.

The effect of the inoculum ratio (15-50%, v/v)), pH (2.5-5.0), temperature (22-35^{o}C), glucose concentration (0.5-3.0%, w/v) and incubation time (4-14 days) were investigated using standard HS medium. To quantify the amount of BC produced, the membranes were placed in the desiccator until constant weight and the dry concentration in grams per liter of culture medium (g/L) was subsequently determined. Results are reported as the mean of duplicate experiments.

2.4. Synthesis of BCC composites

The BCC composites were produced by *Gluconacetobacter* sp. in Hestrin-Schramm medium (HS) containing glucose (2%, w/v), bacto-peptone (0.5%, w/v), yeast extract (0.5%, w/v), disodium hydrogen phosphate (0.27%, w/v), citric acid (0.115%, w/v) and PS clay with concentrations from 0.5 to 20% (w/v). The PS clay was previously smashed and passed through a 40 mesh (140 µM) and retained at a 140 mesh (106 µM).

Main cultivations were carried out at 30^{o}C and pH 3.25 for 7 days under agitated conditions, at 120 rpm. The samples obtained were washed in a 0.5M NaOH solution at 70^{o}C, to remove the bacteria and other impurities, followed by repeated washing with deionized water until the samples had neutral pH. To quantify the amount of BC and BCC produced, the membranes were placed in the desiccator until constant weight and the dry concentration in grams per liter of culture medium (g/L) was subsequently determined. As reference, BC without PS clay was prepared, following the same protocol as for BCC composites.

2.5. Statistical analysis

The statistical analysis of the data was carried using the IBM SPSS Statistics 23 software. Differences in the measurements of a given parameter were assessed by one-way analysis of variance (ANOVA), followed by a Tukey's post hoc analysis. For IGC, the error of the measurements was of 3% and as such the upper and lower values from the experimental value were determined. For the drug release experiments, differences were assessed by a Student's t-test. p-values of <0.05 were considered statistically different.

2.6. BC and BCC composites characterization

2.6.1. Infrared Spectroscopy (FTIR-ATR)

The infrared spectra were obtained using Attenuated Total Reflection Fourier Transform Infrared Spectroscopy (ATR-FTIR) using a Perkin Elmer FTIR System Spectrum BX spectrophotometer equipped with a single horizontal Golden Gate ATR cell after 32 scans in the 4000−500 cm^{-1} range with a resolution of 4 cm^{-1}.

2.6.2. Elemental analysis (EA)

The elemental analysis was performed using a Truspec 630-200-200 elemental analysis equipment under a combustion temperature of 1075ºC, with the aim to identify the chemical compositions of the surface of the samples, determining the weight percentages (%) of elements C, O, N and S.

2.6.3. X-ray diffraction (XRD)

The X-ray diffraction (XRD) measurements were carried out with a Phillips X'pert MPD diffractometer using Cu Kα radiation (λ of 1.54 Å) operating at 45 kV and 40 mA. BC, PS clay and BCC composites with the optimum concentration of incorporated PS clay (8%, w/v) were studied. The 2Θ range under analysis was of 5–70º. The crystallinity index (CI) of the samples was determined through Segal *et al* method [93] according to the following equation:

$$Ic = (1 - \frac{I_{am}}{I_{110}}) \times 100\% \qquad \text{(Equation 10)}$$

Where I_{am} corresponds to the intensities of the amorphous region (18.0º and 13.8º for type I and type II cellulose, respectively) and I_{110} corresponds to the intensity at the (110) plane (22.7º and 21.0º for type I and type II cellulose, respectively).

2.6.4. Scanning electron microscopy (SEM)

Scanning electron micrographs of the surface samples were obtained by Scanning Electron Microscopy (SEM), with a HR-FESEM SU-70 Hitachi equipment operating at 15.0 kV operating in the field emission mode. Samples were deposited on a steel plate and coated with carbon before analysis.

2.6.5. Thermogravimetric analysis (TGA)

Thermogravimetric analysis (TGA) was carried out with a Shimadzu TGA 50 analyzer equipped with a platinum cell. Samples were heated at a constant rate of 10ºC/min, from room temperature to 800ºC, under a nitrogen flow of 20 mL/min.

2.6.6. Swelling ratio (SW)

The swelling ratio (SW) of the membranes was determined by immersing the samples in distilled water at room temperature (minimum of three replicas). The weight increase was periodically measured for 48 hours. BC and BCC composites with concentrations of PS clay from 0.5 to 10% (w/v) were studied. For each measurement, the samples were taken out of the water, wiped dry in filter paper, weighted, and then re-immersed. The SW was calculated using the equation:

$$SW\ (\%) = \frac{W_h - W_d}{W_d} \times 100\% \qquad \text{(Equation 11)}$$

where W_h and W_d are the weights of hydrate and dry membranes, respectively.

2.6.7. Contact angle measurement

A water droplet was aliquoted onto each membrane and the contact angle measurement was recorded with Krüss DSA–100 contact angle analyser, by using on average 10 µL of ultrapure water. The image was processed with the software imageJ using the plug– in *drop_analysis*, using the low–bond axisymmetric drop shape analysis approach (LB–ASDA) developed by Stalder *et al.* [94] BC and BCC composites with the highest incorporation of PS clay (4 and 8%, w/v) were studied.

2.6.8. Inverse Gas Chromatography (IGC)

IGC measurements were carried out on a commercial inverse gas chromatograph (IGC, Surface Measurements Systems, London, UK) equipped with flame ionization (FID) and thermal conductivity (TCD) detectors. The IGC system is fully automatic with SMS IGC

Controller v1.8 control software. Data were analyzed using IGC Standard v1.3 and Advanced Analysis Software v1.25.

BC and BCC composites with the optimum concentration of PS clay (8%, w/v) were packed in the standard glass silanized (dimethyldichlorosilane; Repelcote BDH, UK) columns with 0.2 cm and 30 cm in length by vertical tapping about 2h. The columns with the samples were conditioned 8h at 40°C. After conditioning, pulse injections were carried out with a 0.25 mL gas loop.

Dispersive surface energy measurements were carried using a series of *n*-alkanes, from *n*-octane to *n*-undecane. For specific surface energy measurements, tetrahydrofuran, dichloromethane, ethyl acetate, acetonitrile and acetone were used. In all previous analysis, a concentration of 0.2 p/p_0 was employed. The isotherm measurements of *n*-octane were carried at different concentrations, between 0.05 and 0.2 p/p_0. All measurements were carried with a flow rate of 10 mL/min and at 25–40°C for BC and at 95–110°C for the composites and for PS clay. The higher temperatures applied for the composites and clay powder is due to the strong interactions of the probes with the samples.

The probes were supplied by Sigma Aldrich, with analytic grade (> 99%). Methane was used as an inert reference gas and Helium was used as the carrier gas, both supplied by Air Liquide Company, with a purity above 99%. The physical constants used in IGC were taken from the literature and are displayed in Table 2 [(95)].

Table 2: Physical constants of the applied probes in IGC.

Probe	γ_L^D (mJ/m^2)	a (10^{-19} m^2)	DN (kcal/mol)	AN* (kcal/mol)	γ_L^+ (mJ/m^2)	γ_L^- (mJ/m^2)	χ_t^c
n-heptane	21.3	6.30	-	-	-	-	8
n-nonane	22.7	6.90	-	-	-	-	9
n-decane	23.4	7.50	-	-	-	-	10
n-undecane	246	8.10	-	-	-	-	11
Tetrahydrofuran	22.5	2.90	20.00	0.50	-	-	-
Dichloromethane	24.5	2.45	-	3.90	124.58	0	-
Ethyl acetate	19.6	3.30	17.10	1.50	0	457.67	-
Acetone	16.5	-	17.05	2.51	-	-	-
Acetonitrile	27.5	2.14	14.40	4.70	-	-	-

γ_L^D – Surface tension; a – cross section area; DN – donor number from Gutmann method; AN* - acceptor number from Gutmann method; γ_L^+ - acceptor number from the Van Oss method; γ_L^- - donor number from the Van Oss method; χ_t^c – topological indexes

2.7. Drug incorporation and release studies

To study the incorporation and release kinetics of neomycin sulphate from BC and BCC composites, a calibration curve ranging from 0 to 3 mg/mL was developed.

For drug incorporation studies, BC and an optimum 8% (w/v) BCC hydrogels were immersed in 10 mL water solutions of neomycin sulfate ((1% and (2%, w/v)) followed by mild stirring for 24h, at room temperature.

The *in-vitro* release studies were performed in phosphate buffer saline (PBS, pH 7.4) at room temperature. The loading efficiency and release profiles were obtained by measuring the neomycin sulfate concentration in the collected supernatant by using a UV-6300 PC spectrophotometer (VWR) at 249 nm. For drug detection, a 0.5 mg/mL $CuSO_4.6H_2O$ solution was prepared. These experiments were repeated at least three times for each sample and the average values were collected.

2.8. Antibacterial studies

Antibacterial activity of the BC and BCC composites with the optimum concentration of PS clay (8%, w/v) were studied using disc diffusion method with two strains of bacteria, namely *Escherichia coli* and *Staphylococcus aureus*, and the zone of inhibition was analyzed. Firstly, Luria-Bertani (LB) solid medium and a 0.85% (w/v) NaCl solution were prepared and then autoclaved at 121^{o}C during 15 min.

A qualitative disk diffusion test using 10^6 - 10^7 colony forming units (CFUs) of the *E. coli* and *S. aureus* diluted in 1 mL of 0.85% (w/v) NaCl solution were cultured in Luria-Bertani (LB) agar plates. BC and the optimum BCC composite membranes were kept in two Petri plates cultured with *E. coli* and *S. aureus*. The plates were incubated for 72h at 37^{o}C.

Chapter III – Optimization of culture conditions for BC production

3.1. Optimization of culture medium

With the purpose of optimizing the production of BC by our *Gluconacetobacter* sp., different physiological and nutritional parameters were studied, from which are highlighted: inoculum density, pH, temperature, glucose concentration and production time. The assays for the determination of optimum culture conditions were done in duplicate. The optimization tests of the inoculum density, pH and production time were performed at 30^{o}C whereas the tests to determine the optimum temperature for production of BC were carried out at 22, 25, 30 and 35^{o}C under static conditions.

3.1.1. Influence of inoculum density

To study the effect of inoculum density of *Gluconacetobacter* sp., inoculum from 15% to 50% (v/v) was studied for BC production at 30^{o}C and under static conditions. It was observed (Figure 7) the formation of a BC membrane in all inoculum tested and that the differences between the inoculum studied are not significantly different. Thus, 50% inoculum of *Gluconacetobacter* sp. was chosen as the optimum concentration for BC production as it gave 0.45 g/L BC. According to Hornung *et al*[96], for the maximum BC production, the total bacterial cell count is not important, and the significant quantity is the number of cells in the aerobic zone that are producing cellulose. Consequently, it might be expected from the results obtained in the present study that 50% inoculum density of *Gluconacetobacter* sp. provided the ideal number of cells in the aerobic zone.

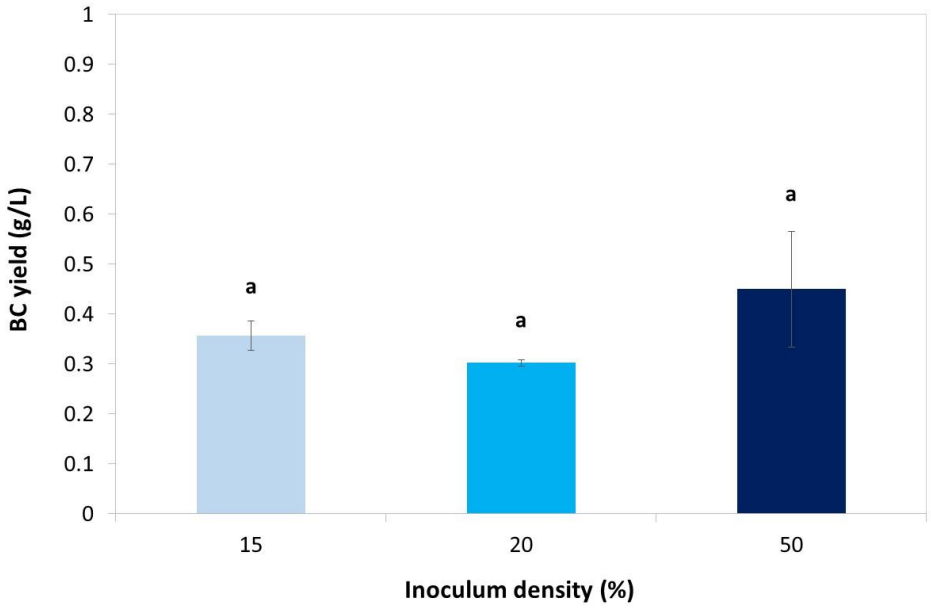

Figure 7*:* Effect of inoculum density on BC production by *Gluconacetobacter* sp.

Values (means) in the same row, not sharing a common superscript are significantly different ($p < 0.05$).

3.1.2. Influence of pH

Since the pH of the culture medium affects the cell growth, this is an important factor which was investigated. Thus, the growth of *Gluconacetobacter* sp. at different pH values, from 2.5 to 5.0 was studied. To study the influence of pH on BC production, the inoculum was adjusted with acetic acid or sodium hydroxide according to the defined values of pH under study. The growth of *Gluconacetobacter* sp. was done at 30ºC, under static conditions.

According to Galas *et al* [97] the optimum pH for BC production depended on the bacterium strain, but has usually been referred to be within a neutral to slightly acidic pH range (4-7). Once the BC production at pH 3.25 and 3.5 were not significantly different, pH 3.25 was selected as the optimum. For a pH of 3.25 this *Gluconacetobacter* strain produced 2.16 g/L BC (Figure 8). Interestingly, this pH value is the one measured when BC production from other species is exhausted, as BC production is stopped or the process becomes less efficient.[24] It is also evident from the results (Figure 8) obtained that at above this pH value, BC production decreased and no BC production was observed at pH 2.5 and 3.0. Comparatively to this study, *Gluconacetobacter medellensis* strain reached a maximum BC production in acidic medium (4.5 g/L), at pH 3.5.[29]

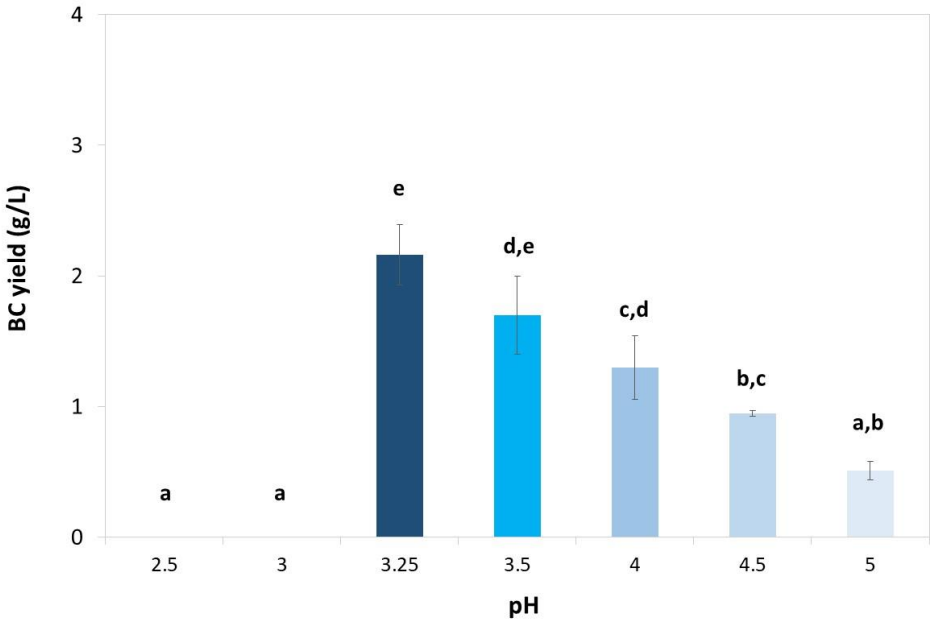

Figure 8: Effect of pH on BC production by *Gluconacetobacter* sp.

Values (means) in the same row, not sharing a common superscript are significantly different ($p < 0.05$).

The results obtained also show a tendency to a decline in the biosynthesis of BC as the pH of the culture medium increases, which is explained by the oxidation of glucose to gluconic acid[98], which lowers the pH and, consequently, inhibits BC production (Figure 8) and decreases the thickness of the membranes. The appearance of culture medium and of the BC membranes can be observed in Figure 9. With the increase in the pH value the thickness of the membranes decreased. Additionally, the medium colour became darker which might be due to the formation of by-products resulting from the metabolism of *Gluconacetobacter* sp.

Remarkably, the strain investigated in this work yields a relatively large amount of BC even in pH 3.25 media, indicating its tolerance to extremely acidic environments while optimally producing BC. As reported by Kim *et al* [27] and Chen *et al* [99], this represents a highly desirable situation in industrially fermentation processes for BC production as it limits microbial contamination since most microorganisms are not viable in low pH media.

Figure 9: Medium colours of *Gluconacetobacter* sp. from pH 3.25 to 5.0.

Additionally to this study, the final pH of the culture medium and the absorbance at 600 nm were measured by UV/Vis (Table 3). For an initial pH of 2.5 it was observed a slight increase in the final pH of the culture medium and a low number of bacteria cells, which demonstrates that the growth of *Gluconacetobacter sp*. was inhibited by the extremely acidic conditions. At a pH of 3.0 the number of bacteria cells increased substantially, but no BC production was observed. On the contrary, at a pH of 3.25 the number of cells grown are lower, but the BC production was higher. Furthermore, the number of cells grown at 3.25 are higher than at a pH of 3.5, supporting the fact that this could be the optimum pH for BC production by *Gluconacetobacter* sp. With an increase to more alkaline conditions, from 3.0 to 5.0, the amount of BC produced by *Gluconacetobacter* sp. decreased substantially mainly due to the formation of gluconic acid, which is responsible for the inhibition of BC production (Figure 9).[98] The final pH of the culture medium decreased until an optimum value for BC production (pH 3.25). Thus, the production of BC by *Gluconacetobacter* sp. is also pH dependent since it affected bacterial growth.

Table 3: Initial and final pH of culture medium and absorbance at 600 nm.

Initial pH	Final pH	Initial Absorbance	Final Absorbance
2.50	2.56		0.26
3.00	2.95		2.20
3.25	3.19		1.87
3.50	3.43	0.44	1.19
4.00	3.77		1.79
4.50	4.34		2.07
5.00	4.80		2.12

3.1.3. Effect of temperature

In the present study, after optimizing pH, the optimum temperature for maximum BC production was optimized (Figure 10). *Gluconacetobacter* sp. was grown at different temperatures (22, 25, 30 and 35°C). To study the influence of the temperature on BC production, the inoculum was adjusted to pH 3.25 with acetic acid.

Results showed that at 30°C *Gluconacetobacter* sp. grew faster and produced 2.95 g/L BC (Figure 10). Minimum BC production was observed at 22°C (0.368 g/L). Similarly to this study, Jahan *et al* [98] studied BC production by *Gluconacetobacter* sp. F6 in temperature range from 20 to 40°C and observed the optimum temperature for BC production to be 30°C.

In addition to the pH of the culture medium, the yield of BC obtained is also temperature dependent. It is an essential parameter that affects both the cell growth and BC production.

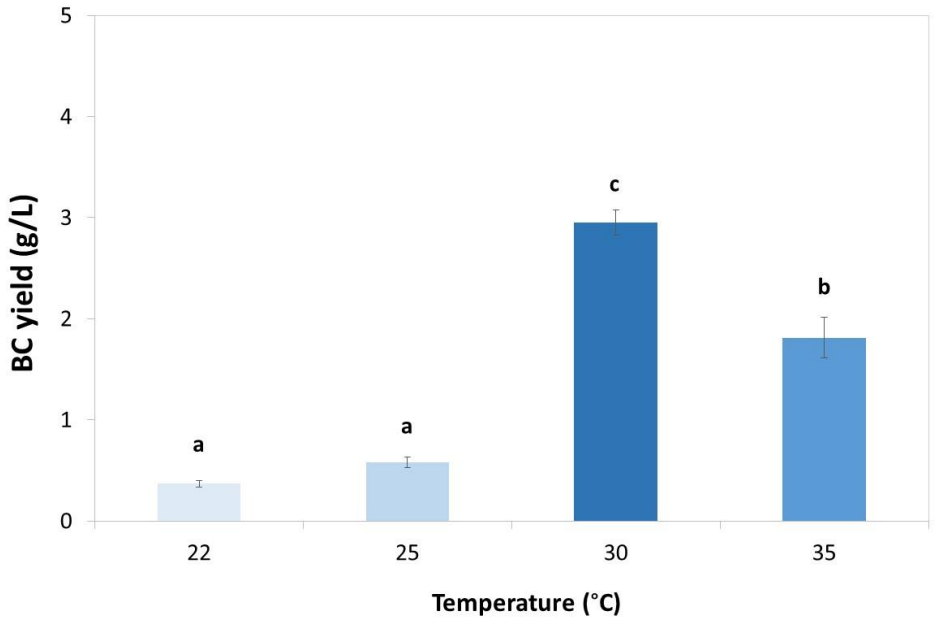

Figure 10: Effect of temperature on cellulose production by *Gluconacetobacter* sp.

Values (means) in the same row, not sharing a common superscript are significantly different ($p < 0.05$).

3.1.4. Effect of glucose concentration

The influence of different glucose concentrations in BC production was investigated in incubations with glucose concentrations from 5 to 30 g/L, an initial pH of 3.25 and a temperature of 30ºC. Results presented in Figure 11 show that with an increase of glucose concentration up to 20 g/L, *Gluconacetobacter* sp. was able to produce the optimum amount of BC (2.95 g/L). It was also observed that on increasing the glucose concentration to 30 g/L, the pH of culture decreased (2.91) and, consequently, inhibited BC production (1.098 g/L). Similar observations were also described by Son *et al* [100] and Masaoka *et al*.[101] The explanation behind lower cellulose production at higher concentration of glucose is that the *Gluconacetobacter* cells oxidize a part of glucose to gluconic acid which lowers the pH of the culture medium and inhibits BC production.[98]

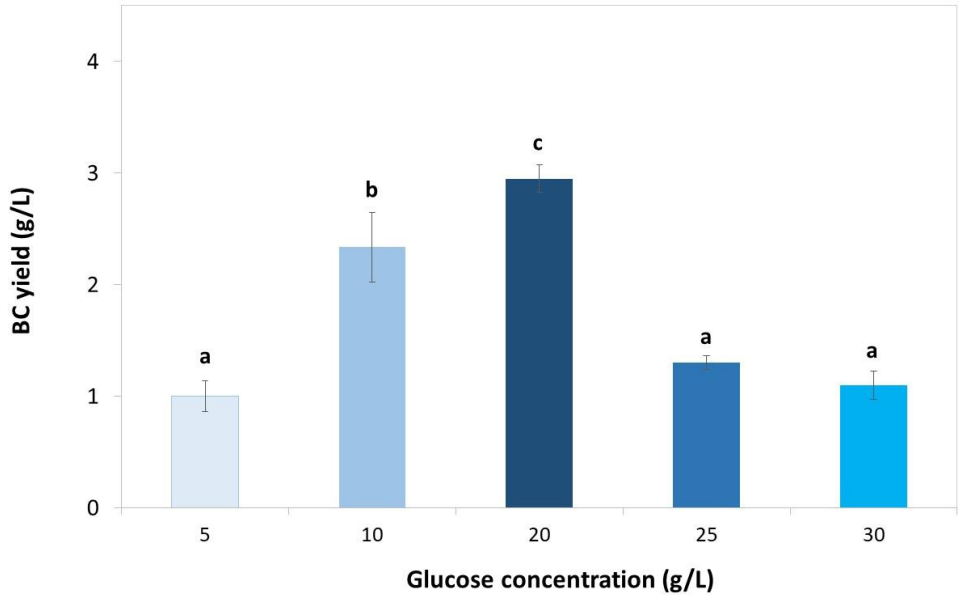

Figure 11: Effect of glucose concentration on BC production by *Gluconacetobacter* sp.

Values (means) in the same row, not sharing a common superscript are significantly different ($p < 0.05$).

3.1.5. Effect of production time

After optimizing the different culture conditions, an optimum Hestrin and Schramm culture medium for BC production was obtained, which contained 2% (w/v) glucose, 0.5% (w/v) peptone, 0.5% (w/v) yeast extract, 0.27% (w/v) disodium hydrogen phosphate, 0.115% (w/v) citric acid and 0.4% (w/v) ethanol, pH 3.25, 30ºC and 50%

inoculum (v/v). Furthermore, the time of BC production by *Gluconacetobacte*r sp. in the optimum medium was studied. BC production was carried out for time periods ranging from 4 to 14 days in static conditions.

As shown in Figure 12, after 4 days of incubation, 1.17 g/L of BC was produced, and the amount of BC produced gradually increased with time. Since the BC production from 7 to 14 days was not significantly different, 7 days were selected as the optimum for BC production (2.95 g/L).

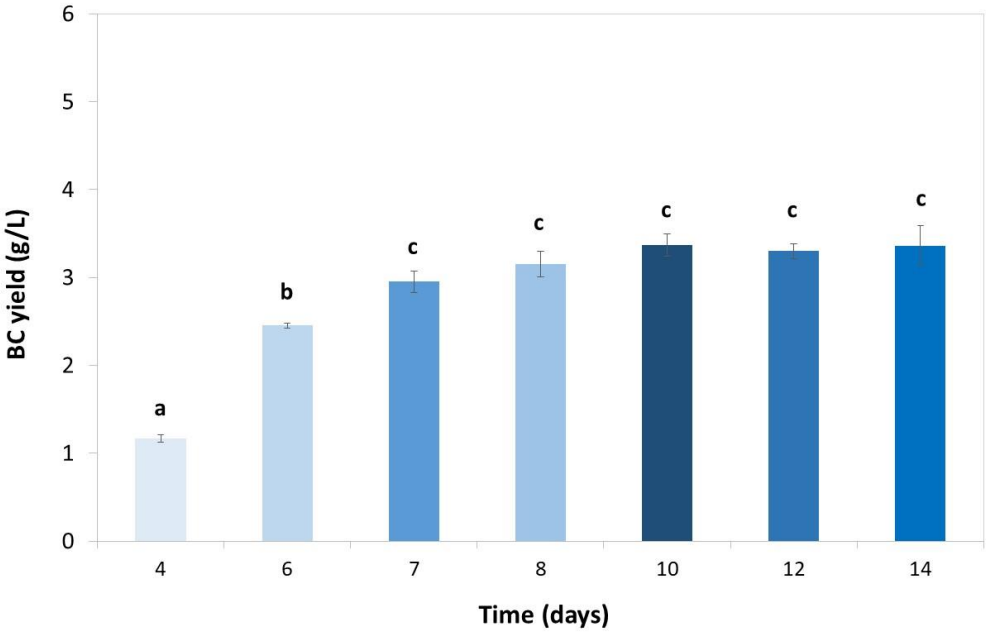

Figure 12: Effect of production time on BC production by *Gluconacetobacter* sp.

Values (means) in the same row, not sharing a common superscript are significantly different ($p < 0.05$).

Chapter IV - Biosynthesis of BCC composites

4.1. Preparation of BC composites

In this study, novel composites of BC and PS clay were produced by *in-situ* biosynthesis in the form of a membrane during the incubation of *Gluconacetobacter sp.* in agitated culture, using a culture medium containing different concentrations of PS clay as outlined in Figure 13.

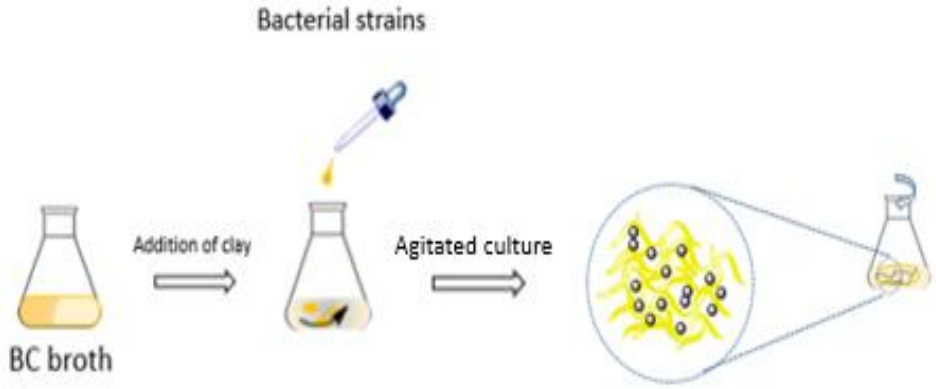

Figure 13: Biosynthesis scheme depicting the *in-situ* biosynthesis of BCC composites.

As particles of PS clay in a static culture sedimented on the bottom of the culture medium so an agitated culture method was applied to provide a better environment for added clay to become entrapped in the BC three-dimensional network due to the constant movement in the medium, which prevented the particles from settling. BCC composites with concentrations of PS clay from 0.5 to 20% (w/v) were synthetized by agitated culture for 7 days at 30ºC (Figure 14). These composites resulted in materials with high clay content as the amount of clay added to the culture media increased (Figure 14). Algar *et al* [(102)] obtained similar results for BC/montmorillonite (MMT) in agitated culture medium where higher MTT content was incorporated into the composites as the MTT content in the BC culture medium increased.

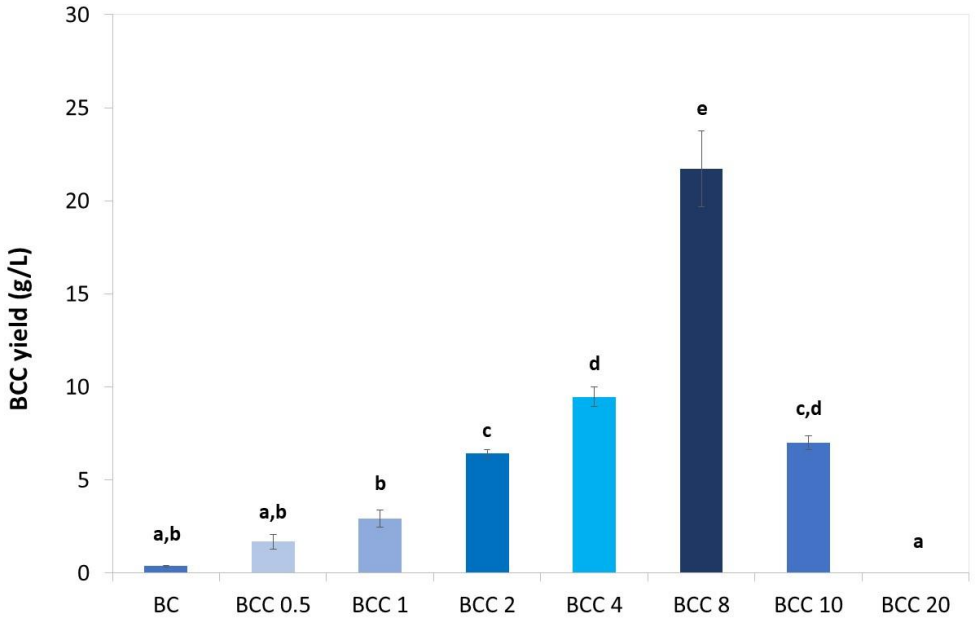

Figure 14: Influence of different concentrations of PS clay (0.5 – 20%, w/v) in the biosynthesis of BCC composites.

Values (means) in the same row, not sharing a common superscript are significantly different ($p < 0.05$).

A considerable amount of BCC (9.47 g/L) was produced at a concentration of PS clay of 4% (w/v). With an increasing concentration of 8% (w/v) there was obtained the optimum amount of BCC (21.73 g/L). At higher concentrations of PS clay, the biosynthesis of BCC composites declined due to the saturation of the culture medium. At a concentration of PS clay of 20% (w/v) it was not observed the formation of a BCC membrane. Furthermore, the membranes of the produced BCC composites became more brittle and with a dark brown coloration (Figure 15).

Figure 15: BCC composite membrane with an optimum concentration of PS clay of 8% (w/v).

Thus, the concentration of PS clay added to the culture medium affected the amount of clay adsorbed onto the surface and inside the BC membranes. Theoretically, the higher the concentration of the clay suspension, the greater will be the number of particles attaching to BC. However, in this work, a very high concentration of PS clay (10 and 20%, w/v) resulted in the agglomeration of particles and saturation of the culture medium, which adversely affected the formation of the composites and their properties.

4.2. BCC characterization

4.2.1. FTIR-ATR Analysis

FTIR-ATR analysis was performed to confirm the incorporation of PS clay into the BC network. Figure 16 shows the FTIR-ATR spectra of BC and BCC composites with different clay contents. The FTIR-ATR spectra of BC show characteristic bands at about 3347 cm^{-1} and 2899 cm^{-1} for stretching vibrations of O-H and C-H, respectively. The presence of the CH group was further supported by its bending vibration at 1430 cm^{-1}. Other important peak that appeared at around 1064 cm^{-1} are due to the stretching vibration of ether groups (C-O-C), which are found within the glucopyranose ring. Regarding the PS clay spectrum, the most prominent bands can be found in the region from 3400 to 3700 cm^{-1}. This spectrum, showed a sharp peak at 3622 cm^{-1} due to the OH stretching and another broad peak centred at 3356 cm^{-1} due to interlayer O-H stretching arising, presumably, from $Mg_2(OH)$ groups of the clay, as previously obtained by Ul-Islam *et al* [103] , after synthetizing BC-MMT composites. Concerning the FTIR-ATR spectra of BCC composites, it showed the presence of characteristic peaks both from BC and PS clay. The OH peak of pure PS clay at 3600 cm^{-1} is present while the broad band near the same region (3400 cm^{-1}) arises due to the merging peaks for the hydrogen bonding of both BC and PS clay. It also shows that with the incorporation of PS clay, the organic-inorganic hydrogen bonding interactions established between the hydroxyl groups of both BC and PS clay become weaker, as well as the chemical bonds of the ether groups of the glucopyranose ring of BC. Additionally, the fingerprint region showed a peak at around 700 cm^{-1} which arises, probably, due to the bending vibration of Mg-O of the PS clay.

In a nutshell, the FTIR-ATR spectra give clear evidence of the formation of the BCC composites. Furthermore, they also displayed the hydrogen bonding interaction between the OH groups of the constituent materials in the composites.

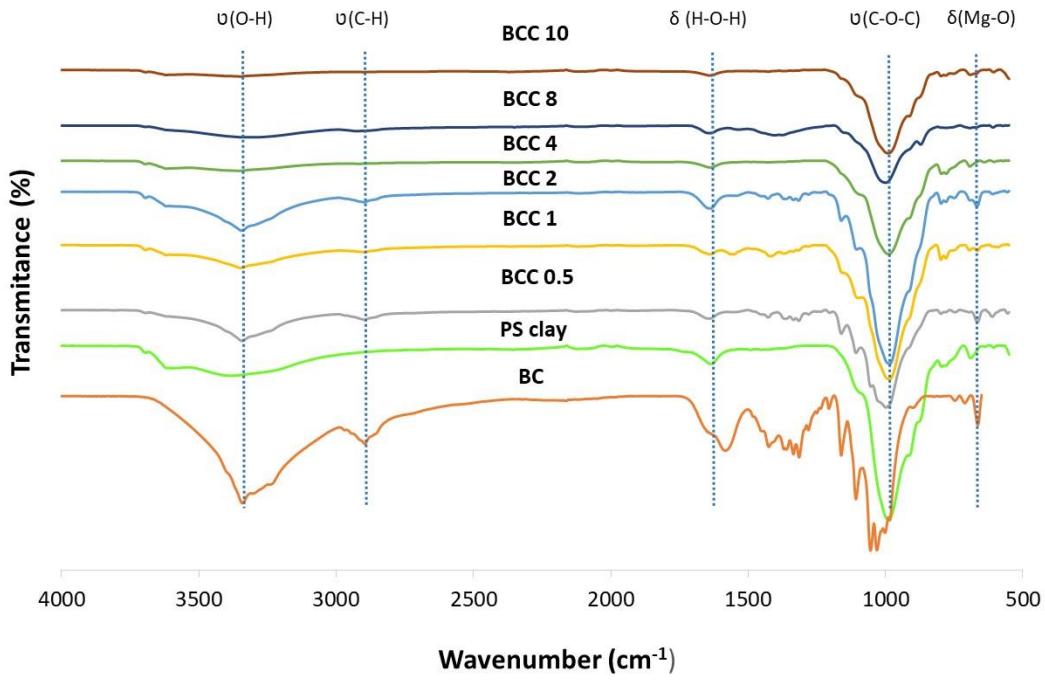

Figure 16: FTIR-ATR spectra of BC, PS clay and BCC composites with concentrations of PS clay from 0.5 to 10% (w/v).

4.2.2. Elemental analysis (EA)

Elemental analysis was employed aiming to evaluate the chemical composition of the samples. In Table 4, that displays the data, it is possible to detect C, O and N. BC, PS clay (PS clay) and BCC composites with the highest incorporation of PS clay were studied. BC presented traces of N, indicating the existence of culture medium impurities. Clays from Porto Santo presented a composition rich in O compared to the percentages of C and N. Additionally, the presence of PS clay on the surface of the composites is evidenced by the presence and increase of O, along with a decrease on the amount of C, corroborating the data obtained from FTIR-ATR and IGC. Regarding the BCC composites, the percentage of N decreased which might be explained by the presence of impurities, that influenced the final concentration of N. Additionally, the percentage

of C in the composites decreased (86-98%), showing that both composites are essentially composed by inorganic elements.

Table 4: Elemental analysis data of BC, PS clay and BCC composites with concentrations of PS clay of 4 and 8% (w/v).

Sample	Elemental composition (%)				
	C	O	N	S	C/O ratio
BC	42.72 [a]	49.95 [a]	1.70 [a]	n.d.	0.86 [a]
PS Clay	0.27 [b]	98.28 [b]	0.03 [b]	n.d.	0.00 [b]
BCC 4	5.93 [b]	91.65 [c]	0.30 [b]	n.d.	0.06 [b]
BCC 8	0.77 [b]	97.27 [b]	0.10 [b]	n.d.	0.01 [b]

Values (means) in the same column, not sharing a common superscript are significantly different ($p < 0.05$). n. d. – not detected; BC – bacterial cellulose; PS Clay – Porto Santo clay; BCC 4 and BCC 8 – BC/clay composites with concentrations of PS clay of 4 and 8% (w/v)

4.2.3. X-ray diffraction (XRD)

The incorporation of PS clay during the biosynthesis of BC can affect its production since it is an amorphous material which could change the crystallization of BC. The XRD technique is an adequate tool to study the crystalline structure, crystal size, the arrangement of the crystals, the distance between the planes of the crystals and the ratio of crystalline and amorphous regions.[104] It also allows the monitoring of the structural changes induced in a crystalline material by blending with semi-crystalline or amorphous materials.[103] In the present study, XRD analysis were carried out in order to investigate the structural changes in BC caused by the adsorption and incorporation of PS clay and to study the crystallinity index of the samples. The XRD patterns of BC, PS clay and BCC composites are shown in Figure 17. The BCC composites with an optimum concentration of PS clay were studied.

The XRD spectrum of BC showed a XRD profile of cellulose type I, with two distinct peaks which appeared at 14.7º and 22.8º. The crystallinity of BC was 71.6%, which is inside the values found on literature, such as the ones reported by Phisalaphong *et al*.[57] (75.2%), Ul-Islam *et al*.[103] (63.2%) and Algar *et al*.[102] (84.9%).

Various diffraction peaks at 2Θ angles of around 19.8º, 26.6º, 27.5º and 35.0º can be found in the XRD spectra of PS clay. On the other hand, Ul-Islam *et al* [103] reported

that MMT (montmorillonite) showed diffraction peaks at around 8.5°, 17.7°, 26.5° and 45.5°. PS clay gives a peak at 19.8° that might be due to the interlayer distance between the silicate sheets of PS clay particles. Comparatively to this work, Gunister *et al* [105] reported that chitosan-MMT composites presented a prominent peak found in the lower angle region corresponding to clay material.

The major diffraction peaks for BC can't be observed in the spectrum of the BCC composites due to its high amorphous content. Additionally, the major diffraction peaks from PS clay can be observed in the spectrum of the BCC composites, which clearly indicates the formation of the composites and supports the SEM and FTIR-ATR structural confirmations. As shown in Figure 17, a slight increase in peak intensity could be found with the incorporation of PS clay in the composites. This might be caused by the agglomeration of clays in the composites as reported previously for the polymer/clay composites. [106]

The attachment and interaction of clay particles disturbed the native hydrogen bonding interactions in BC and resulted into a breaking of the crystalline network of BC and in the formation of composites with high amorphous contents. Therefore, these results confirm the incorporation of PS clay in the 3D network of BC.

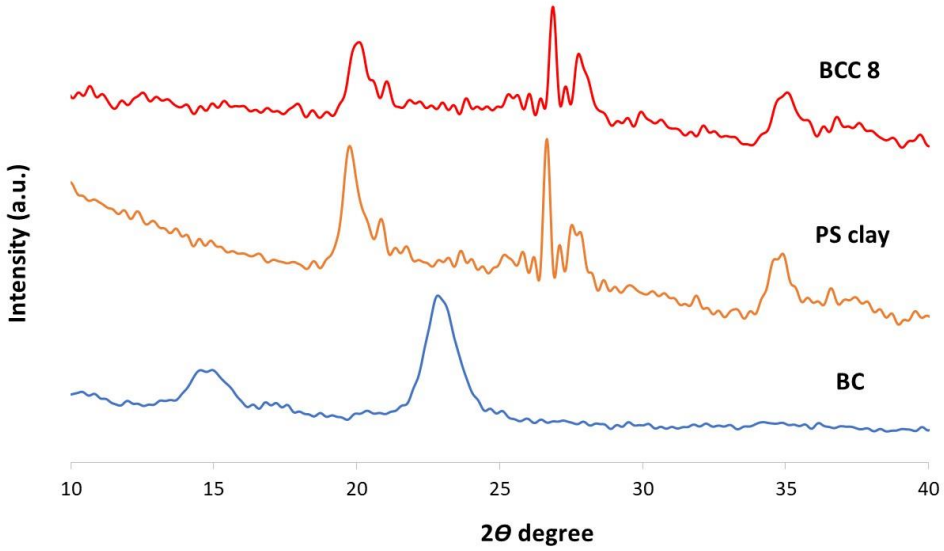

Figure 17: X-ray diffraction profile of BC, PS clay and BCC composites with a concentration of PS clay of 8% (w/v).

4.2.4. Scanning Electron Microscopy (SEM)

The morphological properties of BC and BCC composites with the highest incorporation of PS clay (4 and 8%, w/v) were studied by SEM analysis for characterizing the composites structure and to confirm the biosynthesis of BCC composites. Additionally, SEM was also employed to know the state of dispersion of the particles, penetration into BC and the interactions established between the particles and BC.

The SEM micrographs of BC and BCC composites illustrate a three-dimensional arrangement of the microfibrils (Figure 18). In the case of BC, loosely packed cellulose nanofibrils forming different cellulose layers can be observed, whereas a more compact structure is observed in the BCC composites. BC exhibits a typical cellulose I_β structure, being characterized by the formation of small fibres, which makes its structure more thermodynamically stable. As can be observed (Figure 18), the surface of the composites became less smooth comparing to BC, with the presence of clay flakes on the surface. In both BCC composites, a more compact surface is observed which indicates that the PS clay incorporation filled the pores of BC. The SEM micrographs of BC and BCC composites provide further details of the composite's structures. The particles that penetrated the pores of BC have filled the empty space in the entire matrix. Additionally, the density of clay particles penetrated and accumulated in the matrices of the BCC composites were increased with increasing the concentration of PS clay (Figure 18). The empty spaces between the pores are almost filled in the case of the BCC composite with a concentration of PS clay of 4% (w/v) whereas the pores of the BCC composite with a concentration of PS clay of 8% (w/v) are fully covered.

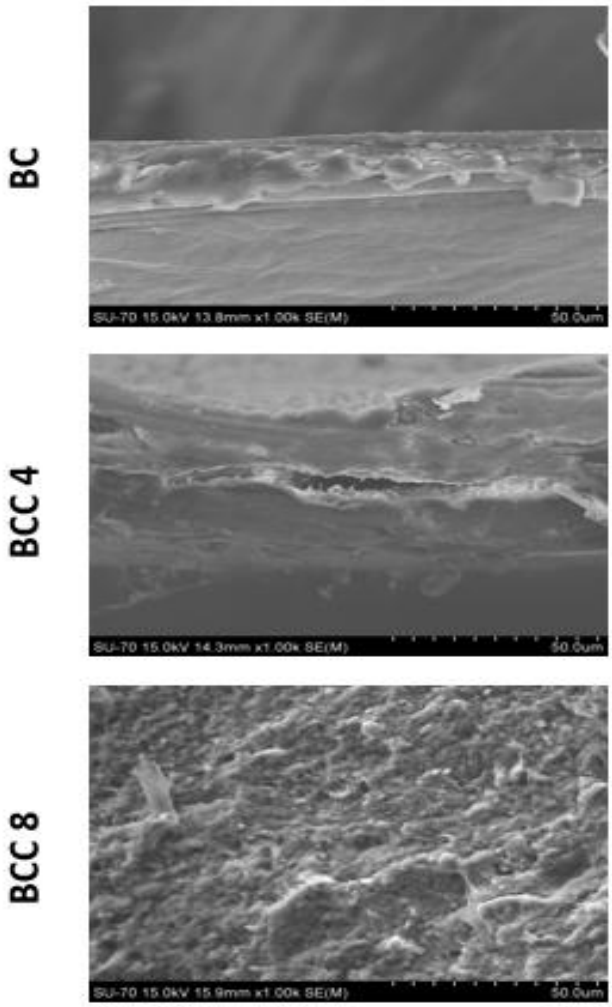

Figure 18: SEM micrographs of BC and BCC composites with concentrations of PS clay of 4 and 8% (w/v).

4.2.5. Thermogravimetric analysis (TGA)

The thermal stability of BC, PS clay and BCC composites with the highest incorporation of PS clay (4 and 8%, w/v) were studied by thermogravimetric analysis. It is known that the thermal stability of BC is influenced by various structure parameters such as crystallinity, molecular weight, orientation of the fibres, dehydration, decarboxylation and depolymerization.[107]

About 5.4% weight loss for BC occurred until temperature of 125°C (Figure 19). On the other hand, the BCC composites showed 6-8.9% weight loss in the same temperature range. The weight loss occurring at 125°C is due to the loss of moisture content and interlayer coordinated water molecules. The relatively higher weight loss

for the BCC composites may be due to the high hydrophilic nature of PS clay. The second phase of degradation starts above 200°C for BC and BCC4 composite due to the degradation of the main cellulose skeleton. The weight loss for BC is about 66% during this phase (Figure 19), which decreases for the BCC composites. For the BCC4 composite, a second degradation peak is nearly absent, where most of the sample was degraded on the first region, whereas for the BCC8 composite the second phase of degradation doesn't occur due to its high thermal stability.

The onset degradation temperature is an important parameter in TGA analysis since it gives information about the thermal stability of BC and BCC composites. Lower onset temperatures indicate that the thermal decomposition starts sooner, corresponding to a less stable material. BC presented an onset temperature of 213.1°C whereas the BCC4 composite presents a higher onset temperature (250.3°C), which evidences a higher thermal stability that might be due to changes in chain orientation.

The thermal degradation profile of the samples could be evaluated by their dTGA curves, where the peak minimum corresponds to the maximum temperature degradation (T_{max}). The main degradation step of BC presented a T_{max} at 297.1°C, which is lower compared to the values found in literature for other BC matrixes (350-360°C) [18, 108], whereas for the BCC4 composites the T_{max} value is similar to BC (296.6°C). The residue of BC at 800°C was 2.1%, which means that the removal of the culture medium impurities was relatively effective. The residue of the BCC composites at the same temperature increased substantially (82.5% and 84.6% for BCC composites with concentrations of PS clay of 4 and 8% (w/v), respectively), indicating the incorporation of clays into the 3D network of BC. The values of the residue of both BCC composites are inside the values of PS clay incorporated (96.2 and 98.3%).

These results indicate that the incorporation of PS clay into the 3D network of BC during the biosynthesis improved the thermal stability of BC. This might be because its presence inside and on the surface of BC can protect the cellulose chains against thermal shock. Therefore, this protection results in shifting the degradation towards higher temperatures and the consequent reduction in the weight loss. Furthermore, the hydrogen bonding established between the BC and oxide groups of PS clay may also improve the thermal properties of the BC chains.

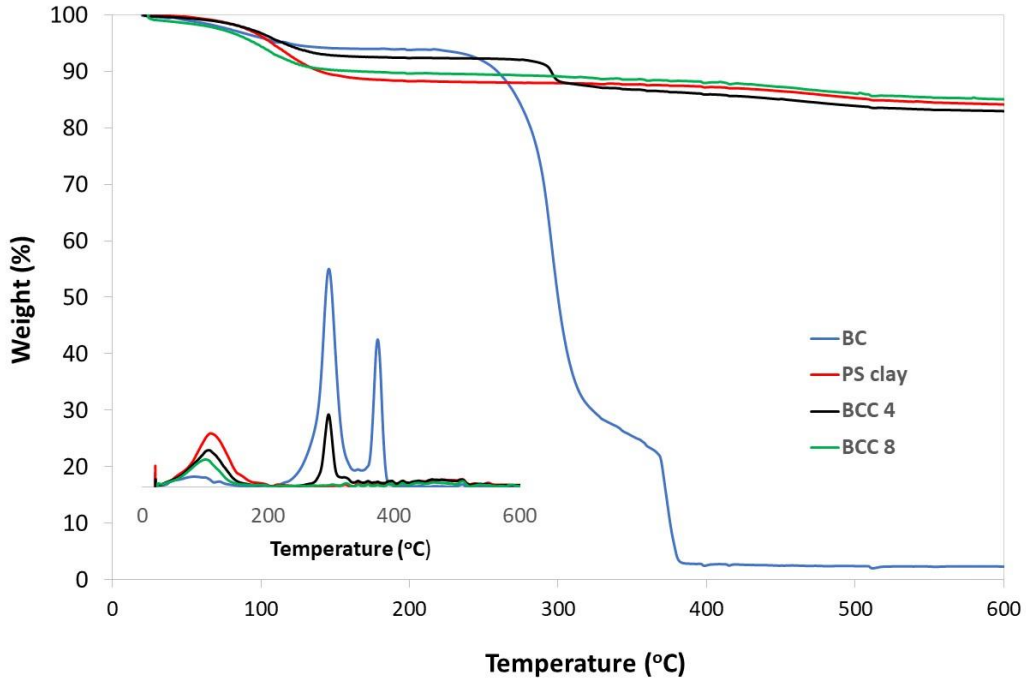

Figure 19: Thermogravimetrical analysis (TGA and dTGA) of BC and BCC composites with concentrations of PS clay of 4 and 8% (w/v).

4.2.6. Swelling ability and contact angle analysis

Nowadays the maintenance of an ideal moisture in wound healing processes is crucial for keeping the wound moist for longer time because it provides a better attachment of active substances to the wound site and warrants a painless wound dressing change without causing damage to the newly formed skin.[103, 109] BC has been extensively studied as a wound dressing material due to its high water holding capability (WHC).[109, 110] However, these properties could be modified by changing the BC structural features or by the incorporation of materials into the BC culture medium for the preparation of its composites. Therefore, the swelling ability of BC and BCC composites were investigated.

The overall results (Figure 20, Table 5) revealed that the BCC composites display a lower swelling ability when compared with BC after 48h of immersion. Additionally, the swelling ability of the composites raised with increasing concentrations of PS clay reaching its maximum at a concentration of 8% (w/v). Above 8% (w/v) the capacity of the composites to retain water decreased due to the saturation of the BCC membranes.

BC presents a steady swelling ability until 7h, reaching a SW_{max} of 670% (Figure 20, Table 5). In case of the BCC composites with concentrations of PS clay of 0.5, 1,2, 4,8 and 10% (w/v), the swelling stabilization occurs at the same time (7h), but presenting much lower SW_{max}, of 267%, 270%, 570%, 281%, 327% and 139%, respectively. For BC, the rehydration ability was the highest obtained, being statistically different compared to the BCC composites ($p < 0.05$). The BCC composites with 10% (w/v) of PS clay presented the lowest swelling ability (139%).

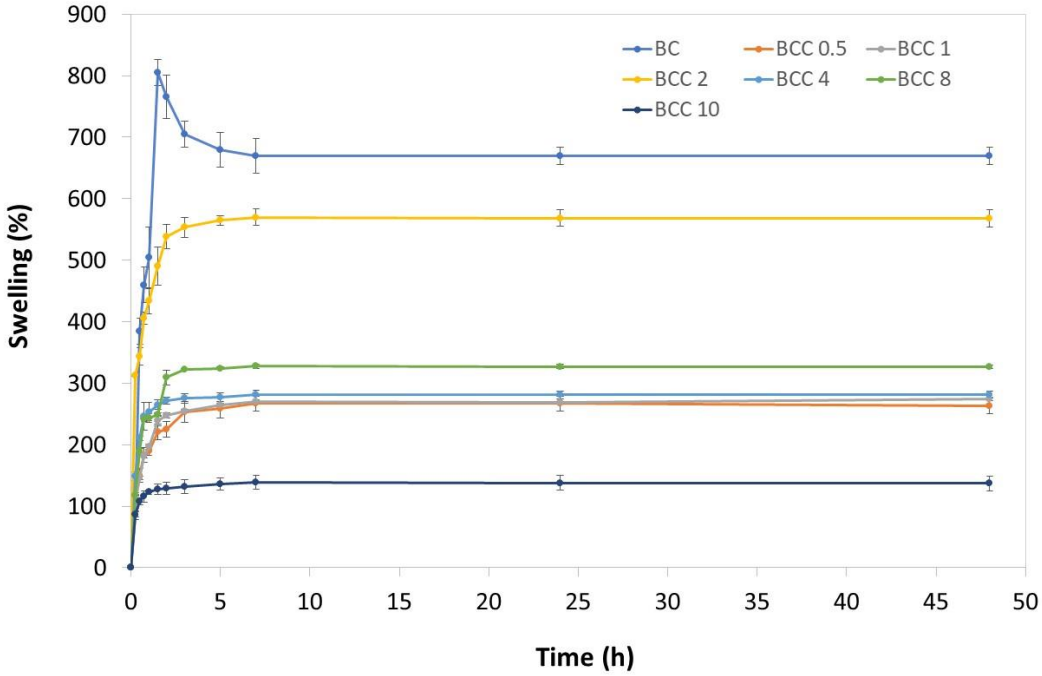

Figure 20: Swelling behaviour of BC and BCC composites during 48 h.

Table 5: Swelling maximum (Sw_{max}) and contact angle of BC and BCC composites with concentrations of PS clay of 4 and 8% (w/v).

	BC	**BCC 4**	**BCC 8**
Sw_{max} (%)	670 ± 4 [a]	281 ± 3 [b]	327 ± 1 [c]
Contact angle (°)	67 ± 3 [a]	24 ± 0.3 [b]	20 ± 1 [b]

Values in the same row, not sharing a common superscript are significantly different ($p < 0.05$).

Additionally, the contact angle measurements were performed for the BC and BCC composites with the highest incorporation of PS clay (4 and 8%, w/v) to evaluate changes in their hydrophilicity (Figure 21). BC showed a contact angle of 67.1º, which is higher than the values reported in the literature (32.6º, 35.4º and 36.9º).[111-113] This might be due to the structural organization of the glucopyranose ring, namely due to a higher number of C-H groups located in the axial positions of the ring. BCC composites with concentrations of PS clay of 4 and 8% (w/v) presented a contact angle much lower (24.3º and 19.7º) than the value obtained for BC, which indicates a higher hydrophilic behaviour. The contact angle measurement of the BCC composites agrees with the swelling maximum obtained, where the samples with higher swelling presented lower contact angle. This fact shows that a more hydrophilic behaviour of the BCC composites is related to a higher water uptake of the samples.

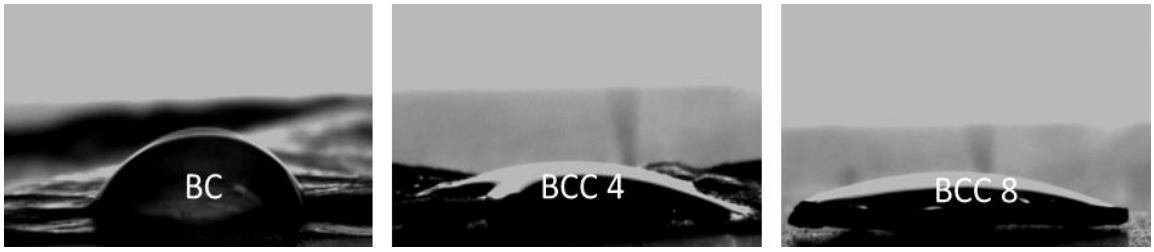

Figure 21: Contact angle analysis of BC and BCC composites with concentrations of PS clay of 4 and 8% (w/v).

4.2.7. Surface properties by IGC

To study the effect of the *in-situ* biosynthesis method, as well as the effect of the incorporation of PS clay on the surface of BC, IGC was applied. Through this technique, the surface energy, acid-basic character and surface morphology of BC and BCC composites were assessed. The acid-base behaviour of the composites was evaluated through the ΔG_s^{sp} and the K_a and K_b values. For the surface morphology studies, the S_{BET} and diffusion parameter (*Dp*) were determined.

4.2.7.1. Surface energy

To study the alterations of surface energy in BC with the incorporation of PS clay (PS clay), BCC composites with the highest incorporation of PS clay were selected.

According to Castro *et al* [31] and Ferguson *et al* [114], BC has a surface energy ($\gamma_s{}^d$) of 39.6 and 42.3 mJ/m^2 at 20^{o}C and 30^{o}C, respectively. In this work, BC had a $\Upsilon_s{}^d$ close to the two values mentioned initially. Table 6 describes the surface energy values of the BC and BCC composites. PS clay presented a $\Upsilon_s{}^d$ inside those obtained by Price *et al* [115] for kaolinite (156-212 mJ/m^2 at 120^{o}C) and by Hamdi *et al* [116] for bentonite (155 mJ/m^2 at 100^{o}C).

Table 6: Surface energy (γ_s^d), ΔG_s^{sp} ratio, acid and basic constants (K_a and K_b) and acid-basic behaviour (K_b/K_a) of bacterial cellulose (BC) at 25^{o}C and of PS clay and BCC composites with concentrations of PS clay 4 and 8% (w/v) at 110^{o}C.

Sample	γs^d(mJ/m^2)	ΔGs^{sp} (DCM/THF)	K_a	K_b	K_b/K_a
BC	42.5 [a]	0.8 [a]	0.09 [a]	0.23 [a]	2.6 [a]
PS clay	178.2 [b]	1.3 [b]	0.21 [b]	0.70 [b]	3.3 [b]
BCC 8	200.2 [b]	0.9 [a]	0.18 [b]	0.75 [b]	4.2 [b]

Values (means) in the same row, not sharing a common superscript are significantly different ($p < 0.05$).

To understand the reason of the increase of the surface energy values, the *n*-octane heterogeneity of the samples was studied, which gives indications of the energy and the number of surface active sites. The energy of the active sites is given by the x axis whereas the number of active sites is observed in the y axis. An increase in the adsorption potential corresponds to an increase in the energy of the active sites, whereas an increase in the y value corresponds to an increase in the number of active sites.

A significant increase (about 79%) in $\Upsilon_s{}^d$ was observed upon incorporation of clays, indicating an increase in the surface hydrophilicity of BC. This behaviour was also observed with the water contact angle (WCA), since it confirmed a shift to a more hydrophilic surface after the incorporation of PS clay (a decrease in the WCA from 67.1^o to 19.7^o was observed). This can be justified by the cellulose anisotropy. According to

Yamane *et al* (2006) cellulose has two inherently different domains (hydrophilic and hydrophobic). The hydroxyl groups located in the equatorial positions of the glucopyranose rings are responsible for the hydrophilic character of cellulose. Contrariwise, the C-H groups located in axial positions of the ring are responsible for its hydrophobic behaviour. Thus, the significant increase in the hydrophilic character of BC suggests that the incorporation of PS clay affects the structural organization of the glucopyranose ring orientation. Therefore, because of the reaction between the cellulose hydroxyl groups with the oxide groups of PS clay, the parallel cellulose chains are oriented so that the O-H bonds are exposed and become more available on the surface of BC. This organization of the polar groups is reflected in the displacement of the adsorption potential maximum (Figure 22) towards higher energies (11.5 to 28.6 kJ mol $^{-1}$), which indicate that the hydrophilicity increased due to the energy increase of the polar active sites after the incorporation of PS clay.

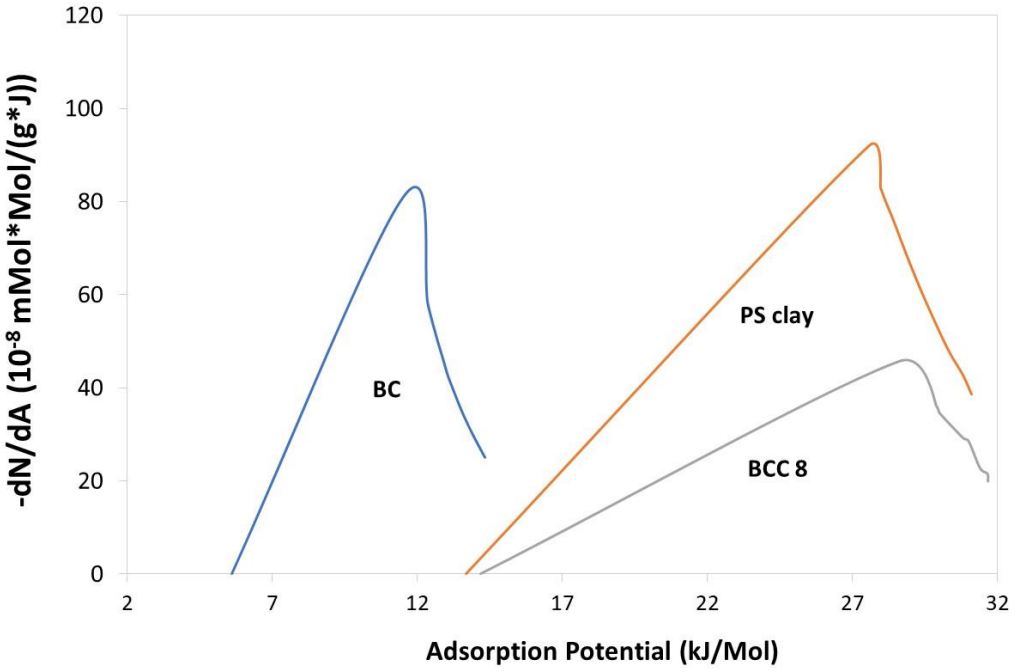

Figure 22: Heterogeneity profile of *n*-octane on BC, PS clay and BCC composites with a concentration of PS clay of 8% (w/v).

4.2.7.2. Acid-base surface character

Through the incorporation of PS clay on the surface of BC, the surface moiety was changed, as revealed by FTIR-ATR. Therefore, the acid-base surface character of the samples was evaluated through IGC.

According to cellulose chemical structure, it was expected an amphoteric behaviour, with a predominantly acidic character, due to the electron acceptors (H from hydroxyl groups) and electron donors (O from glucosidic bonds and hydroxyl groups). (117)

The K_b/K_a ratio of BC shows a basic character (2.6, Table 6) due to arrangement of the hydroxyl groups found at the surface. For PS clay, a higher basic character (3.3, Table 6) is observed, which results from the presence of hydroxyl groups present in PS clay chains (Figure 4). With the attachment of PS clay into the 3D network of BC, the BC basic behaviour is shifted into a more basic behaviour (K_b/K_a of 4.2), which means that there is a higher number of basic groups available in the surface, when compared to BC. Thus, this corroborates the fact that PS clay can be found at the surface of BC. Furthermore, the percentage of O, presented in Table 4, gives an indication of the relative basicity of the BCC composites. The percentage of O is associated with the hydroxyl and oxide groups of Porto Santo clay. When compared to the K_b/K_a values (Table 6), it is seen that the presence of O and lower C is associated with higher K_b/K_a ratios.

To better understand the acid-basic alterations occurred in BC with the incorporation of PS clay, the ΔG_s^{sp} ratio between the acid (dichloromethane) and basic (tetrahydrofuran) probes were studied. Considering the high ΔG_s^{sp} of PS clay (Figure 23), its incorporation onto BC should lead into stronger interactions with the polar probes. Each one of the probes has different energies of interaction since they interact differently with the active sites of the samples surface. The interaction of the surface of BC with tetrahydrofuran (THF) and dichloromethane (DCM) gives an insight about the acid and basic groups present in the surface, respectively.

Regarding BC, the ΔG_s^{sp} of THF is higher than the ΔG_s^{sp} of DCM, giving indication that the surface of BC is basic. With the incorporation of Porto Santo clay on the BC network, there is a slight increase of the ΔG_s^{sp} of THF compared to the ΔG_s^{sp} of DCM,

giving indication of a slightly higher basic behaviour (Figure 23). The ΔG_s^{sp} of acetonitrile (ACN) was the highest obtained among the probes used in this work, which means that it interacted more strongly with the surfaces of the BC, PS clay and BCC composites. Due to its amphoteric nature, it interacts with both acidic and basic groups. This mean that both acidic and basic groups could be found on the surface of BC, PS clay and BCC composites. Thus, through the evaluation of polar probes by IGC it was possible to attest the presence of PS clay in the BCC composites surface.

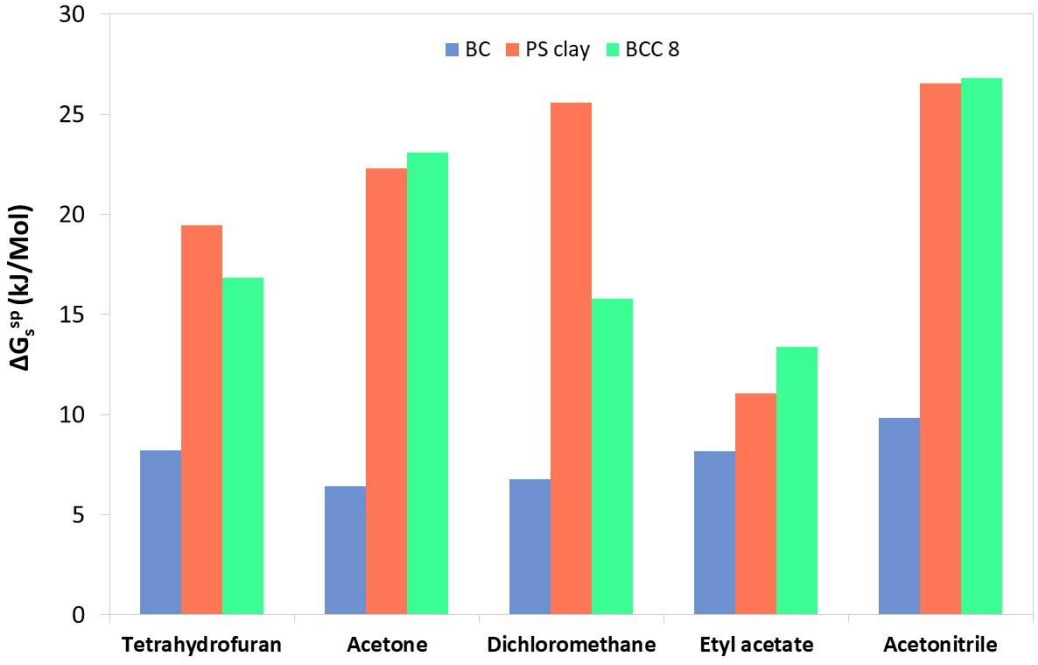

Figure 23: Specific free energy of adsorption (ΔG_s^{sp}) of the polar probes into bacterial cellulose (BC), PS clay and BCC composites with a concentration of PS clay of 8% (w/v).

4.2.7.3. Surface morphology

IGC was also applied to evaluate the surface morphology and the influence of the incorporation of PS clay during the BC biosynthesis.

With the incorporation of clay, the BC S_{BET} is reduced (4%). This decrease is probably due that during composite biosynthesis, clay blocks the surface pores of BC, which not only decrease the area available for probes to access which decreases the S_{BET} but also hinders the crossing of the probes through the sample (lower *Dp*, Table 7).

Through SEM it is observed that the surface becomes more compact (Figure 18), corroborating the IGC results.

Table 7: Surface area (S_{BET}) and diffusion parameter (*Dp*) of BC, PS clay and BCC composites with a concentration of PS clay of 8% (w/v).

Sample	S_{BET} (m^2/g)	Dp (cm/min)
BC	6.32[a]	0.0146[a]
PS clay	8.74[b]	0.0322[c]
BCC8	6.04[a]	0.0022[b]

Values (means) in the same row, not sharing a common superscript are significantly different ($p < 0.05$).

4.3. Drug incorporation and release studies

Neomycin sulphate (Figure 24) is a water soluble aminoglycoside antibiotic and calcium channel protein inhibitor which binds to prokaryotic ribosomes inhibiting translation and is highly effective in topic infections caused by Gram-positive and Gram-negative bacteria, which makes it a broad spectrum drug. [118, 119] It is commonly used to avoid bacterial contamination of cell cultures and in the treatment of eye, skin and gastrointestinal infections. [118]

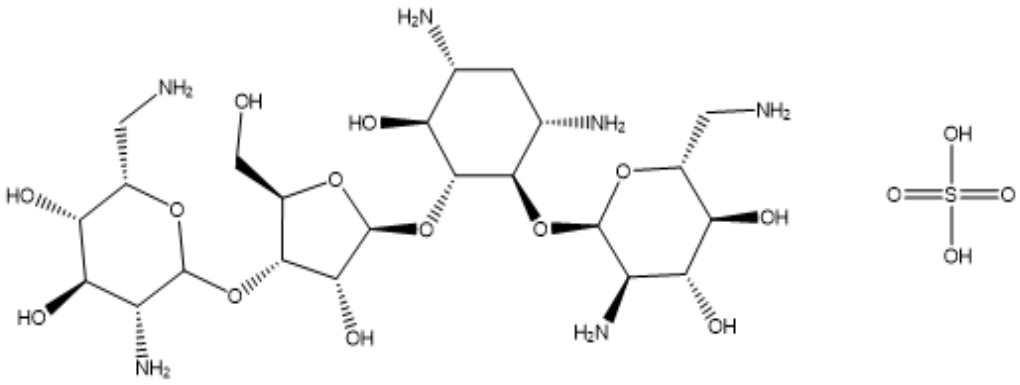

Figure 24: Chemical structure of Neomycin Sulphate.

In this work, for the first time, were investigated the loading onto and release behaviour of neomycin sulphate from BCC composites with 8% (w/v) of PS clay content. The main purpose of the present work was to evaluate the feasibility of BCC composites as potential nanocarriers for controlled drug delivery system, with a prospective application in the treatment of ileum infections and at tissue engineering (wound healing). To this achievement, neomycin sulphate was loaded onto BCC composites as well as BC. The loading efficiency and release profiles were measured and the influence of clay content on the release behaviour of neomycin sulphate was evaluated. For this purpose, a calibration curve of neomycin sulphate ranging from 0 to 3 mg/mL was constructed (Figure 25).

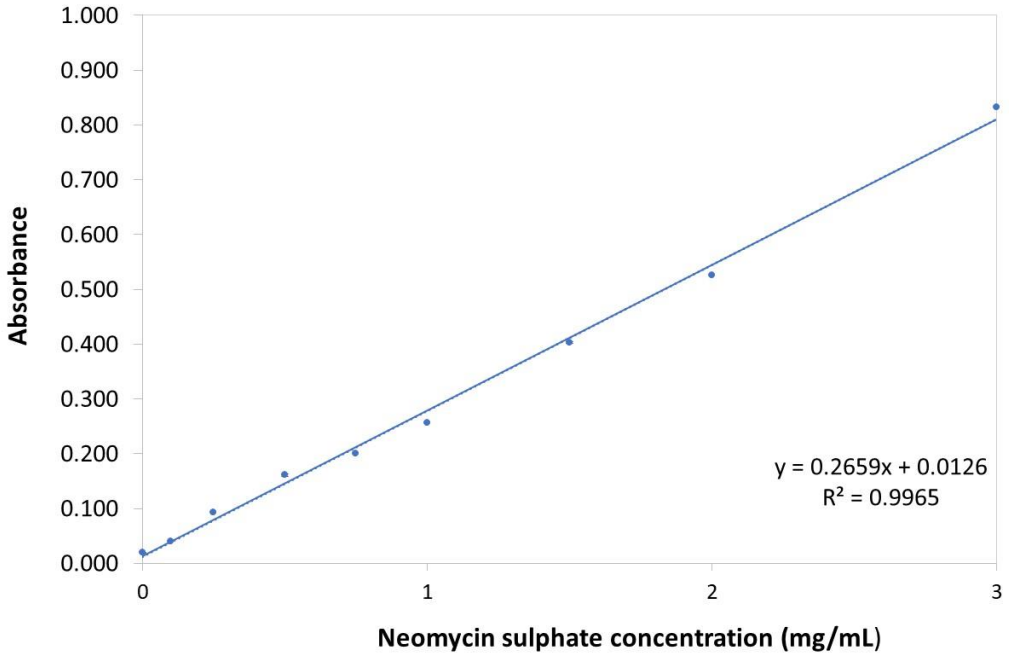

Figure 25: Calibration curve of Neomycin Sulphate.

The drug incorporation tests for BC and BCC composites with 8% (w/v) of PS clay content were carried out with concentrations of neomycin sulphate of 1 and 2% (w/v). The BC and BCC composites showed a higher drug loading capacity with increasing the concentration of neomycin sulphate to 2% (w/v), as shown in Table 8.

Table 8: Drug incorporation efficiency (%) and release (%) of BC and BCC composite membranes with an optimum concentration of PS clay.

Neomycin (%)	Sample	Incorporation efficiency (%)	Drug release (%)
	BC	57.48 [a]	
1	BCC 8	46.64 [a]	-
	BC	73.48 [b]	88.36 [a]
2	BCC 8	72.38 [b]	62.40 [b]

Values (means) in the same row, not sharing a common superscript are significantly different ($p < 0.05$).

The drug release tests for BC and BCC composites with an optimum concentration of PS clay of 8% (w/v) were carried out in phosphate buffer saline (PBS, pH 7.4) and with an optimum neomycin sulphate concentration of 2% (w/v).

As shown in Figure 26, the BC drug release profile shows a fast release behaviour which is typically observed in neutral medium and common for various drug delivery systems.[120] It is noticeable that the BCC composite with 8% (w/v) of PS clay demonstrates a more sustained release as compared to BC in neutral pH. This shows that the BCC composite with 8% (v/v) supports a more sustained and controlled release of neomycin sulphate, making it a suitable drug delivery system. Additionally, the drug release of the BC membranes was higher (88.4%) than for the BCC membranes with 8% (w/v) of PS clay (62.4%), supporting the fact that these composites could be used as drug delivery systems (Table 8).

According to studies developed by Ghadiri *et al* [121] and Wei *et al* [122], laponite and halloysite with encapsulated tetracycline and amoxicillin, respectively were used as controlled and sustained release systems for the treatment of cancer. Additionally, Hamilton *et al* [123] developed antibiotic and antibacterial systems based on different clays (montmorillonite, laponite and kaolinite) and ciprofloxacin composites.

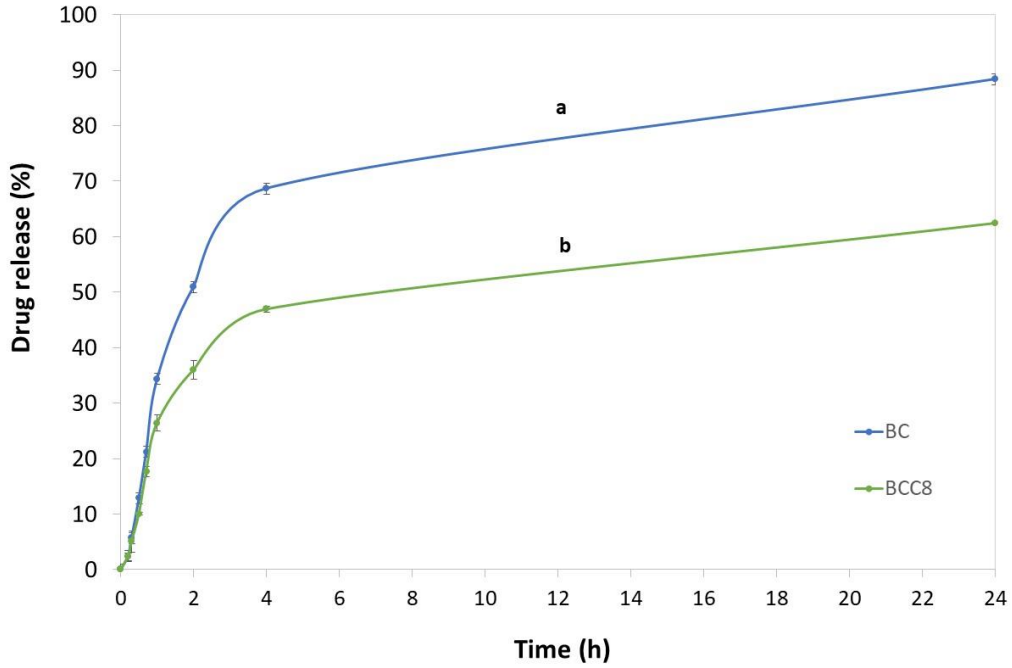

Figure 26: *In-vitro* drug release profiles of BC/neomycin and BCC/neomycin with an optimum concentration of PS clay of 8% (w/v) in pH 7.4, at room temperature.

Values (means) not sharing a common superscript are significantly different ($p < 0.05$).

4.4. Antibacterial studies

In this work, the antimicrobial activities of BC and BCC (8%, w/v) composites with incorporated neomycin sulphate were tested against *Escherichia coli* (Gram-negative) and *Staphylococcus aureus* (Gram-positive) by the agar disc diffusion method.

Regarding this method, the BCC composites with incorporated neomycin exhibited an inhibition zone against both bacteria (Figure 27), while no inhibition zone was observed for the BCC composites without neomycin and for BC. This demonstrated that the antimicrobial activity existed only due to neomycin incorporated inside the BCC composites and not due to BC or to the PS clay incorporated. Additionally, the BCC composites with incorporated neomycin produced a wider inhibition zone against *S. aureus* than *E. coli*. Considering the BCC composites with incorporated neomycin, the BCC composites without drug and the BC membrane, the widths of the inhibition zones of the composite with neomycin were about 2 mm for *S. aureus*, and 1 mm for *E. coli* (Figure 27), respectively, and no inhibition zone was found for BC and for the BCC composite without incorporated neomycin. The antibacterial activity against *E. coli* is

lower than that against *S. aureus*, probably due to the difference in cell walls between Gram-positive and Gram-negative bacteria. The cell wall of the Gram-negative bacteria consists of lipids, proteins and lipopolysaccharides (LPS) that provide effective protection against biocides whereas that of Gram-positive bacteria does not present LPS in its constitution. [124]

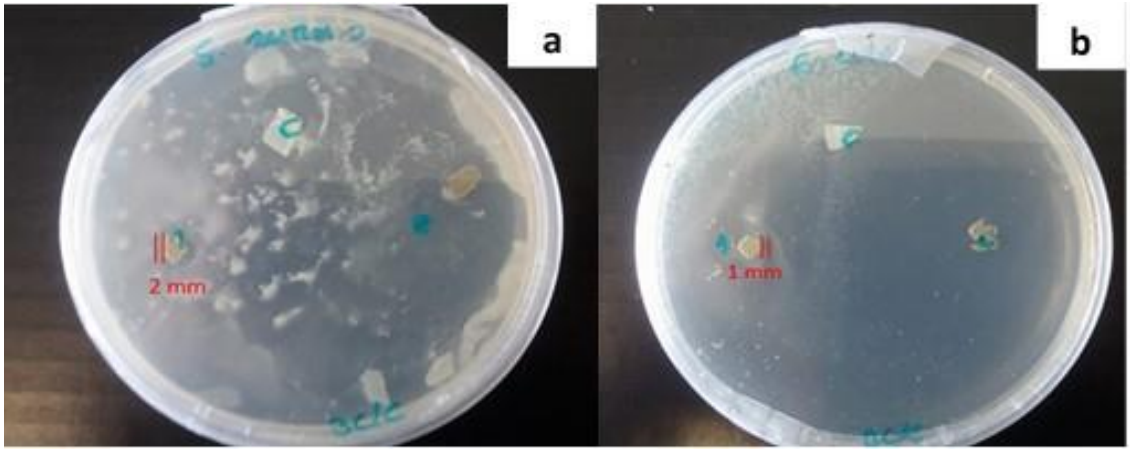

Figure 27: Antimicrobial activity of BC, BCC8 and BCC8 composite with incorporated neomycin sulphate in (**a**) *Staphylococcus aureus* and in (**b**) *Escherichia coli*.

Chapter V – Conclusions and future perspectives

In this work, bacterial cellulose/PS clay composites (BCC) have been obtained by a one-step process, which can be considered an alternative and efficient method for obtaining BC composites with potential applications in drug delivery. Furthermore, the avoidance of organic solvents in this procedure together with the known biocompatible and biodegradable character of both BC and PS clay, expands the possible applications of these materials to the biomedical field as wound dressing materials.

The current study showed that *Gluconacetobacter* sp., presents higher BC producing ability when the pH of the culture medium went above 4. The highest BC production of *Gluconacetobacter* sp. reached 2.95 g/L at optimized culture conditions of: 2% glucose, pH of 3.25, 30^{o}C and 7 days of cultivation. Furthermore, BCC composites where produced at optimum culture conditions of: 2% glucose, 30^{o}C, pH 3.25 and under agitated conditions (120 rpm), for 7 days. An optimum concentration of PS clay of 8% (w/v) produced 21.7 g/L BCC.

The BCC composites were submitted through a series of analysis to evaluate the influence of the clay incorporation in the physico-chemical properties of the resulting material. FTIR-ATR, EA, XRD and TGA provided important information of the successful incorporation of PS clay on BC, which is clearly visible through SEM. The thermal stability (83%) of the BCC composites increased in comparison to BC.

Inverse gas chromatography (IGC) has proven to be a suited technique in the evaluation of the changes occurred in the surface of the BCC composites. It made evident a significant increase in the surface energy (79%) of the BCC composites, as well as a shift to a higher basic surface (Kb/Ka → 4.2), comparatively to BC. Additionally, it was observed changes in the BC morphology due to the incorporation of clay, where the different BCC composites showed lower S_{BET} and Dp, which proofs the influence of PS clay in the properties of the resulting composites.

Based in the widely recognized therapeutic properties of BC and PS clay, BCC composites suggest plenty of opportunities for their medicinal use. The prospect of merging these two non-toxic materials is especially attractive for drug delivery applications, mainly as oral capsules for the treatment of infections of ileum.

The BCC composites were studied in terms of their ability to control the release of neomycin sulphate. These materials exhibited a reduced initial burst effect comparatively to BC and a sustained release up to 24h in a pH 7.4 simulated intestinal fluid. The BCC composites with incorporated neomycin sulphate showed higher antibacterial activity against Gram-positive bacteria (*S.aureus*) than Gram-negative bacteria (*E.coli*). According to these results, these BCC composites can find interesting applications mainly as clinical wound healing materials.

References

1. Sun D, Yang J, Wang X. Bacterial cellulose/TiO_2 hybrid nanofibers prepared by the surface hydrolysis method with molecular precision. Nanoscale. 2010;2(2):287-292
2. Saied H, Diwany A, Basta A, Atwa N, Ghwas D. Production and characterization of economical bacterial cellulose. BioResources. 2008;3(4):1196-1217
3. Mohite B, Patil S. A novel biomaterial: bacterial cellulose and its new era applications. Biotechnology and Applied Biochemistry. 2014;61:101-110
4. Keshk S, Sameshima K. Evaluation of different carbon sources for bacterial cellulose production. African Journal of Biotechnology. 2005;4(6):478-482
5. Keshk S, Razek T, Sameshima K. Bacterial cellulose production from beet molasses. African Journal of Biotechnology. 2006;5(17):1519-1523
6. Carreira P. Produção de celulose bacteriana a partir de resíduos industriais [Tese de Mestrado em Materiais Derivados de Recursos Renováveis]: Universidade de Aveiro; 2010
7. Chawla P, Bajaj I, Survase S, Singhal R. Microbial Cellulose: Fermentative Production and Applications. Food Technology and Biotechnolology. 2009;47(2):107-124
8. Cai J, Kim J. Bacterial cellulose/poly(ethylene glycol) composite: Characterization and first evaluation of biocompatibility. Cellulose. 2010;17:83-91
9. Czaja W, Young D, Kawecki M, Brown R. The Future Prospects of Microbial Cellulose in Biomedical Applications. Biomacromolecules. 2007;8(1):1-12
10. Ross P, Mayer R, Benziman M. Cellulose Biosynthesis and Function in Bacteria. Microbiological Reviews. 1991;55(1):35-58
11. Gardner D, Oporto G, Mills R, Samir M. Adhesion and Surface Issues in Cellulose and Nanocellulose. Journal of Adhesion Science and Technology. 2008;22:545-567
12. Romling U. Molecular biology of cellulose production in bacteria. Research in Microbiology. 2002;153:205-212
13. Dayal M, Goswami N, Sahai A, Jain V, Mathur G, Mathur A. Effect of media components on cell growth and bacterial cellulose production from Acetobacter aceti MTCC 2623. Carbohydrate Polymers. 2013;94:12-16

14. Mohan D, Pittman C, Steele P. Pyrolysis of Wood/Biomass for Bio-oil: A Critical Review. Energy and Fuels 2006;20:848-889

15. Brown R. Cellulose Structure and Biosynthesis: What is in Store for the 21st Century? Journal of Polymer Science Part A: Polymer Chemistry. 2003;42(3):487-495

16. Vieira R. Estudo da eficiência e durabilidade de diversos métodos de fixação de produtos antimicrobianos em fibras celulósicas [Mestrado em Química Têxtil]: Universidade do Minho; 2006

17. Lustri W, Barud H, Peres M, Gutierrez J, Tercjak A. Microbial Cellulose — Biosynthesis Mechanisms and Medical Applications. Cellulose - Fundamental Aspects and Current Trends. 2015:133-157

18. Poletto M, Pistor V, Zattera A. Structural Characteristics and Thermal Properties of Native Cellulose. Cellulose - Fundamental Aspects. 2013;2:45-68

19. Klemm D, Heublein B, Fink H, Bohn A. Cellulose: Fascinating Biopolymer and Sustainable Raw Material. Polymer Science. 2005;44:3358-3393

20. Pecoraro E, Manzani D, Messaddeq Y, Ribeiro S. Bacterial Cellulose from *Gluconacetobacter xylinus*: Preparation, Properties and Applications. 2008;17:369-83.

21. Gao W, Chen K, Yang R, Yang F, Han W. Properties of bacterial cellulose and its influence on the physical properties of paper. BioResources. 2011;6(1):144-153

22. Donini I, De Salvi D, Fukumoto F, Lustri W, Barud H, Marchetto R, *et al*. Biossíntese e recentes avanços na produção de celulose bacteriana Eclética Química. 2010;35(4):165-178

23. Keshk S. Bacterial Cellulose Production and its Industrial Applications. Journal of Bioprocess and Biotechnology 2014;4(2):1-10

24. Klemm D, Schumann D, Udhardt U, Marsch S. Bacterial synthesized cellulose - artificial blood vessels for microsurgery Polymer Science. 2001;26:1561-1603

25. Brown A. On an acetic ferment which forms cellulose. . Journal of Chemical Society. 1886;49:432-439

26. Bergey's Manual of Systematic Bacteriology East Lansing Springer 2005

27. Kim S, Lee S, Park K, Park S, An H, Hyun J, *et al*. *Gluconacetobacter* sp. gel_SEA623-2, bacterial cellulose producing bacterium isolated from citrus fruit juice. Saudi Journal of Biological Sciences. 2017;24:314 -319

28. Yeo, Soo-Hwan, Lee O, Lee I, Kim H, Yu T, *et al*. *Gluconacetobacter persimmonis* sp. nov., Isolated from Korean Traditional Persimmon Vinegar. Journal of Microbiology and Biotechnology. 2004;14(2):276-283

29. Castro C, Zuluaga R, Álvarez C, Putaux J, Caro G, Rojas O, *et al*. Bacterial cellulose produced by a new acid-resistant strain of *Gluconacetobacter* genus. Carbohydrate Polymers. 2012;89:1033-1037

30. Shah N, Islam M, Khattak W, Park J. Overview of bacterial cellulose composites: A multipurpose advanced material. Carbohydrate Polymers. 2013;98:1585-1598

31. Castro C, Cordeiro N, Faria M, Zuluaga R, Putaux J, Filpponen I, *et al*. *In-situ* glyoxalization during biosynthesis of bacterial cellulose. Carbohydrate Polymers. 2015;126:32-39

32. Nakagaito A, Iwamoto S, Yano H. Bacterial cellulose: the ultimate nano-scalar cellulose morphology for the production of high-strength omposites. Applied Physics A: Materials Science & Processing. 2005;80:93-97

33. Yano H, Sugiyama J, Nakagaito A, Nogi M, Matsuura T, Hikita M, *et al*. Optically Transparent Composites Reinforced with Networks of Bacterial Nanofibers Advanced Materials. 2005;17(2):153-155

34. Maeda H, Nakajima M, Hagiwara T, Sawaguchi T, Yano S. Bacterial cellulose/silica hybrid fabricated by mimicking biocomposites. Journal of Materials Science. 2006;41:5646-5656

35. Wan Y, Luo H, He F, Liang H, Huang Y, Li X. Mechanical, moisture absorption, and biodegradation behaviours of bacterial cellulose fibre-reinforced starch biocomposites. Composites Science and Technology. 2009;69:1212-1217

36. Pértile R. Bacterial cellulose: studies on biocompatibility, surface modification and interaction with cells [Tese de Doutoramento em Engenharia Biomédica]: Universidade do Minho; 2010

37. Lee K, Buldum G, Mantalaris A, Bismarck A. More Than Meets the Eye in Bacterial Cellulose: Biosynthesis, Bioprocessing, and Applications in Advanced Fiber Composites. Macromolecular Bioscience. 2014;14:10-32

38. Yano S, Maeda H, Nakajima M, Hagiwara T, Sawaguchi T. Preparation and mechanical properties of bacterial cellulose nanocomposites loaded with silica nanoparticles. Cellulose. 2008;15:111-120

39. Ashjaran A. Properties and Applications of Bacterial Cellulose as a Biological Non-woven Fabric. Asian Journal of Chemistry. 2013;25(2):783-788

40. Vandamme E, De Baets S, Vanbaelen A, Joris K, De Wulf P. Improved production of bacterial cellulose and its application potential. Polymer Degradation and Stability. 1998;59:93-99

41. Cheng K, Catchmark J, Demirci A. Effects of CMC Addition on Bacterial Cellulose Production in a Biofilm Reactor and Its Paper Sheets Analysis. Biomacromolecules. 2011;12:730-736

42. Bielecki S, Krystynowicz A, Turkiewicz M, Kalinowska H. Bacterial Cellulose. Biopolymers Online. 2005;3:37-46

43. Cheng K, Catchmark J, Demirci A. Enhanced production of bacterial cellulose by using a biofilm reactor and its material property analysis. Journal of Biological Engineering 2009;1:3-12

44. Krystynowicz A, Czaja W, Jezierska A, Miskiewicz M, Turkiewicz M, Bielecki S. Factors affecting the yield and properties of bacterial cellulose Journal of Industrial Microbiology and Biotechnology. 2002;29:189-195

45. Hestrin S, Schramm M. Synthesis of Cellulose by Acetobacter xylinum 2. Preparation of freeze-dried cells capable of polymerizing glucose to cellulose Journal of Biochemistry. 1954;58(2):345-352

46. Hu Y. A novel bioabsorbable bacterial cellulose Pennsylvania State University; 2011

47. Jonas R, Farah L. Production and application of microbial cellulose Polymer Degradation and Stability 1998;59:101-106

48. Brown E. Bacterial cellulose/thermoplastic polymer nanocomposites: Washington State University; 2007

49. Iguchi M, Yamanaka S, Budhiono A. Bacterial cellulose - a masterpiece of nature's arts. Journal of Materials Science. 2000;35:261-270

50. Esa F, Tasirin S, Rahman N. Overview of Bacterial Cellulose Production and Application. Agriculture and Agricultural Science Procedia. 2014;2:113-119

51. Budhiono A, Rosidi B, Taher H, Iguchi M. Kinetic aspects of bacterial cellulose formation in nata-de-coco culture system. Carbohydrate Polymers. 1999;40:137-143

52. Slusarska B, Presler S, Danielewicz D. Characteristics of Bacterial Cellulose Obtained from Acetobacter Xylinum Culture for Application in Papermaking. Fibres & Textiles in Eastern Europe 2008;16(4):108-111

53. McKenna B, Mikkelsen D, Wehr J, Gidley M. Mechanical and structural properties of native and alkali-treated bacterial cellulose produced by *Gluconacetobacter xylinu*s strain ATCC 53524. Cellulose. 2009;16(6):1047-1055

54. George J, Ramana K, Sabapathy S, Bawa A. Physico-Mechanical Properties of Chemically Treated Bacterial (*Acetobacter xylinum*) Cellulose Membrane. World Journal of Microbiology and Biotechnology. 2005;21(8-9):1323-1327

55. Knauth P, Schoonma J. Nanocomposites: ionic conducting materials and structural spectroscopies. HL T, editor2008

56. Castro C, Vesterinen A, Zuluaga R, Caro G, Filpponen I, Rojas O, *et al*. *In situ* production of nanocomposites of poly(vinyl alcohol) and cellulose nanofibrils from *Gluconacetobacter* bacteria: effect of chemical crosslinking. Cellulose. 2014;21:1745-1756

57. Phisalaphong M, Jatupaiboon N. Biosynthesis and characterization of bacteria cellulose–chitosan film. Carbohydrate Polymers. 2008;74:482-488

58. Saibuatong O, Jatupaiboon N. Novo aloe vera–bacterial cellulose composite film from biosynthesis. Carbohydrate Polymers. 2010;79:455-460

59. Figueiredo A, Figueiredo A, Silva N, Barros-Timmons A, Almeida A, Silvestre A, *et al*. Antimicrobial bacterial cellulose nanocomposites prepared by *in situ* polymerization of 2-aminoethyl methacrylate. Carbohydrate Polymers. 2015;123:443-453

60. Luo H, Xiong G, Huang Y, He F, Wang Y, Wan Y. Preparation and characterization of a novel COL/BC composite for potencial tissue engineering scaffolds. Materials Chemistry and Physics. 2008;110:193-196

61. Grande C, Torres F, Gomez C, Bañó M. Nanocomposites of bacterial cellulose/hydroxyapatite for biomedical applications. Acta Biomaterialia. 2009;5:1605-1615

62. Mohammadkazemi F, Faria M, Cordeiro N. *In situ* biosynthesis of bacterial nanocellulose-$CaCO_3$ hybrid bionanocomposite: One-step process. Materials Science and Engineering C. 2016;65:393-399

63. Williams L, Haydel S. Evaluation of the medicinal use of clay minerals as antibacterial agents. International Geology Review. 2010 52(7-8):745-770

64. Yang J, Lee J, Ryu H, Elzatahry A, Alothman Z, Choy J. Drug–clay nanohybrids as sustained delivery systems. Applied Clay Science. 2016;130:20-32

65. Zeynabad F, Salehi R, Mahkam M. Design of pH-responsive antimicrobial nanocomposite as dual drug delivery system for tumor therapy. Applied Clay Science. 2017;141:23-35

66. Jafarbeglou M, Abdouss M, Shoushtari A, Jafarbeglou M. Clay nanocomposites as engineered drug delivery systems. Royal Society of Chemistry Advances. 2016;6:1-15

67. Williams L. Geomimicry: harnessing the antibacterial action of clays. Clay Minerals. 2017;52:1-24

68. Pena - Ferreira M, Santos D, Silva J, Amaral M, Sousa - Lobo J, Gomes J, *et al*. Aplicação de argilas esmectíticas da ilha do Porto Santo em máscaras faciais. Anales de Hidrologia Medica. 2011;4:67-79

69. Mansa R, Dzene L, Quintela A, Rocha F, Detellier C. Preparation and characterization of novel clay/scleroglucan nanocomposites. Applied Clay Science. 2016;126:235-244

70. Cordeiro N, Silva J, Gomes C, Rocha F. Bentonite from Porto Santo Island, Madeira archipelago: surface properties studied by inverse gas chromatography. Clay Minerals. 2010;45:77-86

71. Voelkel A, Strzemiecka B, Adamska K, Milczewska K. Inverse gas chromatography as a source of physiochemical data. Journal of Chromatography A. 2009;1216:1551-1566

72. Al Saigh Z. Review: inverse gas chromatography for the characterization of polymer blends. Int J Polym Anal Charac. 1997;3:249-291

73. Rückriem M, Inayat A, Enke D, Gläser R, Einicke W, Rockmann R. Inverse gas chromatography for determining the dispersive surface energy of porous silica. Colloids and Surfaces A: Physicochemical and Engeneering Aspects. 2010;357:21-26

74. Thielmann F. Introduction into the characterisation of porous materials by inverse gas chromatography. Journal of Chromatography A. 2004;1037:115-123

75. Conder J. Physicochemical measurements: gas chromatography. Science EoS, editor. Detroit, USA: Academic Press; 2000

76. Cordeiro N, Ashori A, Hamzeh Y, Faria M. Effects of hot water pre-extraction on surface properties of bagasse soda pulp. Materials Science and Engineering C. 2013;33:613-617

77. Rani P, Ramanaiah S, Reddy K. Lewis acid-base properties of cellulose acetate butyrate by inverse gas chromatography. Surface Interface Analysis. 2011;43(3):683-688

78. Mukhopadhyay P, Schreiber H. Aspects of acid-base interactions and use of inverse gas chromatography. Colloids and Surfaces A: Physicochemical and Engineering Aspects. 1995;100:47-71

79. Mohammadi-Jam S, Waters K. Inverse gas chromatography applications: a review. Advances in Colloid and Interface Science. 2014;212:21-44

80. James A, Martin J. Gas-Liquid partition chromatography: the separation and micro-estimation of volatile fatty acids from formic acid to dodecanoic acid. Biochemical Journal. 1952;50:679-690

81. Domínguez J, Díez-Masa J. Retention parameters in Chromatography. Pure and Applied Chemistry. 2001;73:969-992

82. Al-Saigh Z. Review: inverse gas chromatography for the characterization of polymer blends. International Journal of Polymer Analysis Characterization. 1997;3:249-291

83. Fowkes F. Attractive forces at interfaces. Industrial & Engineering Chemistry. 1964;56:40-52

84. Schultz J, Lavielle L, Martin C. The role of the interface in carbon-fibre epoxy composites. Journal of Adhesion. 1987;23:45-60

85. Goss K. Considerations about the adsorption of organic moelcules from the gas phase to surfaces: implication for inverse gas chromatography and the prediction of adsorption coefficients. Journal of Colloid and Interface Science. 1997;90:241-249

86. Riddle F, Fowkes F. Spectral shifts in acid-base chemistry. 1 - Van der Waals contributions to acceptor numbers. Journal of the American Society. 1990;112:3259-3264

87. Walton K, Snurr R. Applicability of the BET method for determining surface areas of microporous metal-organic frameworks. Journal of American Chemical Society. 2007;129:8552-8556

88. Balard H. Estimation of the surface energetic heterogeneity of a solid by inverse gas chromatography. Langmuir. 1997;13:1260-1269

89. Sen A. Inverse gas chromatography. India: Defense Scientific Information & Documentation Centre; 2005

90. Ghazali M, Nawawi M. Diffusion coefficient estimations by thin-channel column inverse gas chromatography: preliminary experiments. Pertanika Journal of Science and Technology. 2000;8(1):1-18

91. Jackson P, Huglin M. Use of inverse gas chromatography to measure diffusion coefficients in crosslinked polymers at different temperatures. European Polymer Journal. 1995;31(1):63-65

92. Phisalaphong M, Jatupaiboon N. Biosynthesis and characterization of bacteria cellulose. Carbohydrate Polymers. 2008;74(3):482-488

93. Segal L, Creely J, Martin Jr A, Conrad C. An Empirical Method for Estimating the Degree of Crystallinity of Native Cellulose Using the X-Ray Diffractometer. Textile Research Journal. 1959;29:786-794

94. Stalder A, Kulik G, Sage D, Barbieri L, Hoffmann P. A snake-based approach to accurate determination of both contact points and contact angles. Colloids and Surfaces A: Physicochemical and Engeneering Aspects. 2006;286:92-103

95. Cordeiro N, Gouveia C, Moraes A, Amico S. Natural fibers characterization by inverse gas chromatography. Carbohydrate Polymers. 2011;84:110-117

96. Hornung M, Ludwig M, Gerrard A, Schmauder H. Optimizing the Production of Bacterial Cellulose in Surface Culture: Evaluation of Substrate Mass Transfer Influences on the Bioreaction (Part 1). Engineering in Life Sciences. 2006;6:537-545

97. Galas E, Krystynowicz A, Tarabasz-Szymanska L, Pankiewicz T, Rzyska M. Optimization of the production of bacterial cellulose using multivariable linear regression analysis. Engineering in Life Sciences. 1999;19(3):251-260

98. Jahan F, Kumar V, Rawat G, Saxena R. Production of Microbial Cellulose by a Bacterium Isolated from Fruit. Journal of Applied Biochemistry and Biotechnology. 2012;167:1157-1171

99. Chen X, Lou W, Zong M, Smith T. Optimization of culture conditions to produce high yields of active *Acetobacter* sp. CCTCC M209061 cells for anti-Prelog reduction of prochiral ketones. BMC Biotechnology. 2011;11:1-12

100. Son H, Heo M, Kim Y, Lee S. Optimization of fermentation conditions for the production of bacterial cellulose by a newly isolated *Acetobacter* sp. A9 in shaking cultures. Biotechnology and Applied Biochemistry. 2001;33:1-5

101. Masaoka S, Ohe T, Sakota N. Production of cellulose from glucose by *Acetobacter xylinum*. Journal of Fermentation and Bioengineering. 1993;75(1):18-22

102. Algar I, Garcia-Astrain C, Gonzalez A, Martin L, Gabilondo N, Retegi A, *et al*. Improved Permeability Properties for Bacterial Cellulose/Montmorillonite Hybrid Bionanocomposite Membranes by *In-Situ* Assembling. Journal of Renewable Materials. 2016;4(1):57-65

103. Ul-Islam M, Khan T, Kon Park J. Nanoreinforced bacterial cellulose-montmorillonite composites for biomedical applications. Carbohydrate Polymers. 2012;89:1189-1197

104. Pavlidou S, Papaspyrides C. A review on polymer-layered silicate nanocomposites. Progress in Polymer Science. 2008;33:1119-1198

105. Gunister E, Pestreli D, Unlu C, Atici O, Gungor N. Synthesis and characterization of chitosan-MMT biocomposite systems. Carbohydrate Polymers. 2007;67(3):358-365

106. Akat H, Tasdelen M, Du Prez F, Yagci Y. Synthesis and characterization of polymer/clay nanocomposites by intercalated chain transfer agent. European Polymer Journal. 2008;44(7):1949-1954

107. Lin S, Huang Y, Hsu K, Lai Y, Chen Y, Cheng K. Isolation and identification of cellulose-producing strain *Komagataeibacter intermedius* from fermented fruit juice. Carbohydrate Polymers. 2016;151:827-833

108. Liu Z, Wang H, Lu X, Zhang X, Zhang S, Zhou K. Characterization of the regenerated cellulose films in ionic liquids and rheological properties of the solutions. Materials Chemistry and Physics. 2011;128(1-2):220-227

109. Shezad O, Khan S, Khan T, Kon Park J. Physicochemical and mechanical characterization of bacterial cellulose produced with an excellent productivity in static conditions using a simple fed-batch cultivation strategy. Carbohydrate Polymers. 2010;82:173-180

110. Ul-Islam M, Shah N, Hwan Ha J, Kon Park J. Effect of chitosan penetration on physico-chemical and mechanical properties of bacterial cellulose. Korean Journal of Chemistry and Engineering. 2011;28(8):1736-1743

111. Silva C, Bottene M, Barud H, Barud H, Ligabue R, Jahno V. Wettability and Morphological Characterization of a Polymeric Bacterial Cellulose/corn Starch Membrane. Materials Research. 2015;18:109-113

112. Lee K, Blaker J, Bismarck A. Surface functionalisation of bacterial cellulose as the route to produce green polylactide nanocomposites with improved properties. Composites Science and Technology. 2009;69:2724-2733

113. Lopes T, Riegel-Vidotti I, Grein A, Tischer C, Faria-Tischer P. Bacterial cellulose and hyaluronic acid hybrid membranes:Production and characterization. International Journal of Biological Macromolecules. 2014;67:401-408

114. Ferguson A, Khan U, Walsh M, Lee K, Bismarck A, Shaffer M, *et al*. Understanding the Dispersion and Assembly of Bacterial Cellulose in Organic Solvents. Biomacromolecules. 2016;17:1845-1853

115. Price G, Ansari D. An inverse gas chromatography study of calcination and surface modification of kaolinite clays. Physical Chemistry Chemical Physics. 2003;5:5552-5557

116. Hamdi B, Kessaissia Z, Donnet J, Wang T. Variation of surface energy of a bentonite by chemical and thermal treatments. Annales de Chimie Science des Materieux. 1999;24:63-73

117. Gamelas J. The surface properties of cellulose and lignocellulosic materials assessed by inverse gas chromatography: a review. Cellulose. 2013;20:2675-2693

118. Abraha A, Gholap A, Belay A. Study Self-association, Optical Transition Properties and Thermodynamic Properties of Neomycin Sulfate Using UV-Visible Spectroscopy International Journal of Biophysics. 2016;6(2):16-20

119. Szaniszlo B, Iuga C, Bojita M. Indirect Determination of Neomycin by Derivative Spectrophotometry. Clujul Medical. 2011;84(3):398-401

120. Knipe J, Peppas N. Multi-responsive hydrogels for drug delivery and tissue engineering applications. Regenerative Biomaterials. 2014;1:57-65

121. Ghadiri M, Hau H, Chrzanowski W, Agus H, Rohanizadeh R. Laponite clay as a carrier for *in situ* delivery of tetracycline. Royal Society of Chemistry Advances. 2013;1(3):20193-20201

122. Wei W, Minullina R, Abdullayev E, Fakhrullin R, Mills D, Lvov Y. Enhanced efficiency of antiseptics with sustained release from clay nanotubes. Royal Society of Chemistry Advances. 2014;4(1):488-494

123. Hamilton A, Hutcheon G, Roberts M, Gaskell E. Formulation and antibacterial profiles of clay-ciprofloxacin composites. Applied Clay Science. 2014;87:129-135

124. Feng Q, Wu J, Chen G, Cui F, Kim T, Kim J. A mechanistic study of the antibacterial effect of silver ions on *Escherichia coli* and *Staphylococcus aureus*. Journal of Biomedical Materials Research. 2000;52(4):662-668